# A STUDY OF THE TORSIONAL CAPACITY OF REINFORCED CONCRETE RECTANGULAR BEAMS

by 1264

JOSEPH CHIA-HUA CHU

B.S. in C.E., Taiwan Provincial Taipei Institute of Technology
1965

---

A MASTER'S REPORT

submitted in partial fulfillment of the

requirements for the degree

MASTER OF SCIENCE

Department of Civil Engineering

KANSAS STATE UNIVERSITY
Manhattan, Kansas

1970

Approved by:

Robert R. Snell

Major Professor

# TABLE OF CONTENTS

LIST OF FIGURES

LIST OF TABLES

# INTRODUCTION

Torsion, which results essentially from the monolithic character of concrete construction is generally considered as a secondary effect in the design of reinforced concrete buildings. In some cases, such as balcony girders, the torque may contribute to the controlling stress in the member. However, the behavior of reinforced concrete beams under pure torque or torque combined with flexural moment is still not clearly understood. Theoretical and experimental research is still being undertaken in an attempt to understand this phenomena. Several theories have been developed, and under certain circumstances, these theories predict the true ultimate load in very good agreement with test results.

In this report, Lessig's theory and Hsu's theory are reviewed. Furthermore, these theories are compared with the results of tests conducted by Mason(12), using small scale models loaded in pure torque. Lessig's theory combines the effect of torque, bending moment and transverse load. However, his general equations can be applied to the pure torque case by setting the bending moment and the transverse load equal to zero.

# REVIEW OF LITERATURE

In 1929, Rausch presented a method for predicting the ultimate resistance of a reinforced concrete rectangular beam being loaded with torque. His method was later modified by Andersen(1) and Cowan(2,3). The Andersen-Cowan theory starts from plain concrete elements analysed by Saint-Venant's theory as well as Prandtl's membrane analogy for both elastic and plastic stress distribution. The stresses caused by twisting moment are divided into a diagonal principal tensile force and a diagonal principal compressive force. The maximum torque that the beam can resist is the torque that would cause tensile failure of the concrete. For larger torques, the excessive principal tensile force is assumed to be taken by the steel reinforcement. This theory was adopted in the 1958 Australian Code. Studying this code, it is found that most of the equations were derived on the bases of elastic stress distribution. However, some concepts of plastic redistribution of shear stress were introduced.

A different theory concerning torque on reinforced concrete beams was proposed by Lessig(4,5,6,7) in 1959. This was considered to be a more reliable theory which explained some observed phenomena prior to failure quite reasonably. The ultimate loads predicted by using the equation derived by her were also in fairly good agreement with test results, provided that the beam failed through the yielding of the longitudinal and transverse reinforcement which intersects the failure surface. Her study included the effect of flexure and transverse force combined with torque.

By 1962, the Portland Cement Association Laboratory began some research on a torsional theory for rectangular reinforced concrete beams. By comparison of the results of the experimental tests carried out by P.C.A. and results reported by others, Hsu (8,9,10,11) pointed out that there are some discrepancies between Lessig's theory and observed phenomena. In 1968, he suggested a theory in which a different surface of failure was proposed. Based on this failure surface, he derived an equation for rectangular beams under pure torsion.

Small scale model tests can be divided into two categories in both design and research, the direct method and the indirect method. In direct model analysis, the behavior of structures both in the elastic and inelastic ranges can be investigated. In indirect model analysis, only elastic behavior of prototype structures can be examined. These techniques have been developed over the past half century, but the significant use of them as tools in structural design and research has occurred only for the past 10 to 15 years.

An application of small scale model tests to prestressed concrete structure in the inelastic range was carried out by Burton in 1964. In his report, he demonstrated that a mix of Ottowa sand and plaster could have the required compressive strength and demonstrate similar behavior to the concrete used in prototype structures.

In a Master's thesis published in 1965, Cardenas compared the experimental results he obtained, for rectangular reinforced plaster model beams subjected to combined bending and torque, with Lessig's theory. A reasonably good agreement between his results and Lessig's theory was reported.

Mason(12) examined the ultimate resistance of small scale models of rectangular reinforced beams subjected to pure bending and pure torque in 1967. The test results are good for pure bending. But for pure torque, Lessig's theory overestimated the test results. The same type of discrepancy was reported in papers by Yudin in 1962 and Hsu in 1968(11).

## LESSIG'S THEORY FOR PURE TORQUE

In 1956, Lessig, through experimental observations, defined two possible modes of failure for reinforced concrete beams subjected to bending moment, transverse load and torsion. These failure modes are dependent on the ratios between these applied loads. If the beam is subjected to a large flexure moment accompanied by a small twisting moment, the beam fails by the first mode, that is the neutral axis intersects both vertical sides of the beam (Fig. 1). On the other hand, if the beam is subjected to a large torsional moment and a small bending moment, it fails by the second mode, that is the neutral axis intersects both horizontal sides of the beam. (Fig. 2)

A complete theory to explain these failure modes was reported in 1959. (4,5) In these papers, Lessig pointed out that the position of the compression zone, the angle between the neutral axis and beam axis, and the load-bearing capacity depend on:

(1). the magnitude of the forces acting in the beam at the surface of failure.

(2). the steel and concrete properties.

(3). the width as well as the depth of the beam.

(4). the quantities of the longitudinal and transverse reinforcement as well as the ratio between them.

In order to derive the equations, the following assumptions must be made:

(1). when a spatial plastic hinge forms, all steel intersecting the tension part of the failure surface reaches its yield stress.

(2). the tension in the concrete at the surface of failure is completely ignored.

(3). the compressive stress in the concrete at the section under study reaches its ultimate strength as in flexure compression.

(4). the quantity of transverse reinforcement is assumed constant and uniformly distributed over the beam.

(5). no external loads are applied within the length where failure takes place.

Based on the above assumptions and the failure modes that Lessig defined, the ultimate resistance of a beam can be found by the use of equilibrium equations. For pure torque, which is the case to be considered here, the failure mode would have the neutral axis pass through both horizontal faces and

$$M = 0$$

$$Q = 0$$

(see Fig. 3). The moment equilibrium equation about the neutral axis is

$$M_o = T \frac{c}{l} \qquad (1)$$

in which

l - length of the neutral axis.

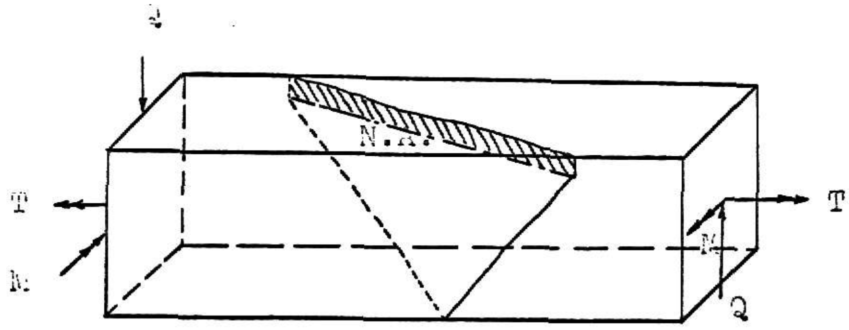


FIG. 1 - FIRST MODE OF FAILURE
DEFINED BY LESSIG

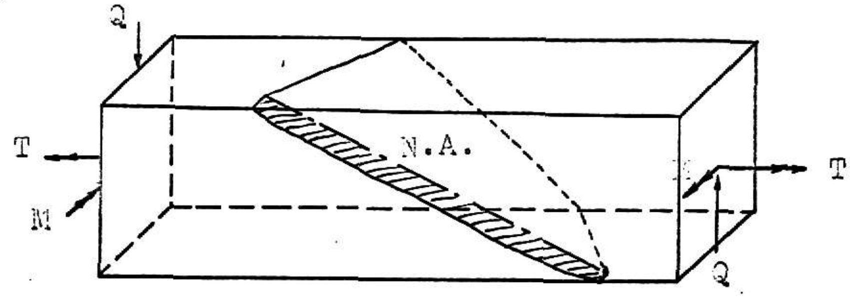


FIG. 2 - SECOND MODE OF FAILURE
DEFINED BY LESSIG

$M_o$ - moment about the neutral axis.

$M_o$ is made up of four parts, designated as $M_1$, $M_2$, $M_3$, and $M_4$. In order to make the derivation straight forward, each part is discussed individually.

A). $M_1$, (due to the compression in the concrete).

$$M_1 = f_c \cdot S_b$$

wherein

$f_c$ - ultimate strength of concrete, can be approximated as the compressive strength in flexure, $0.85f_c'$.

$S_b$ - static moment of compression area about the neutral axis, BC.

refering to Fig. 3c

$$BC = l, \qquad AD = \sqrt{h^2 + c^2}$$

and

$$S_b = \int_A dA \cdot S = \int_A x \cdot d\xi \cdot \left( \frac{x}{2} \cdot \frac{\sqrt{h^2 + c^2}}{l} \right)$$

In this integral, x is a function of $\xi$

$$x = x_1 + (x_2 - x_1) \frac{\xi}{\sqrt{h^2 + c^2}} = \frac{x_1 l' + (x_2 - x_1)\xi}{l'} \qquad (2)$$

Introducing $l' = \sqrt{h^2 + c^2}$.

Substituting $l'$ into the expression for $S_b$,

then

$$S_b = \frac{1}{2l'l} \int_0^{l'} [\, x_1 l' + (x_2 - x_1)\xi \,]^2 d\xi$$

$$= \frac{l'^2}{6l} (x_1 + x_1 x_2 + x_2^2)$$

thus

$$M_1 = \frac{f_c (h^2 + c^2)}{6l} (x_1^2 + x_1 x_2 + x_2^2) \qquad (3)$$

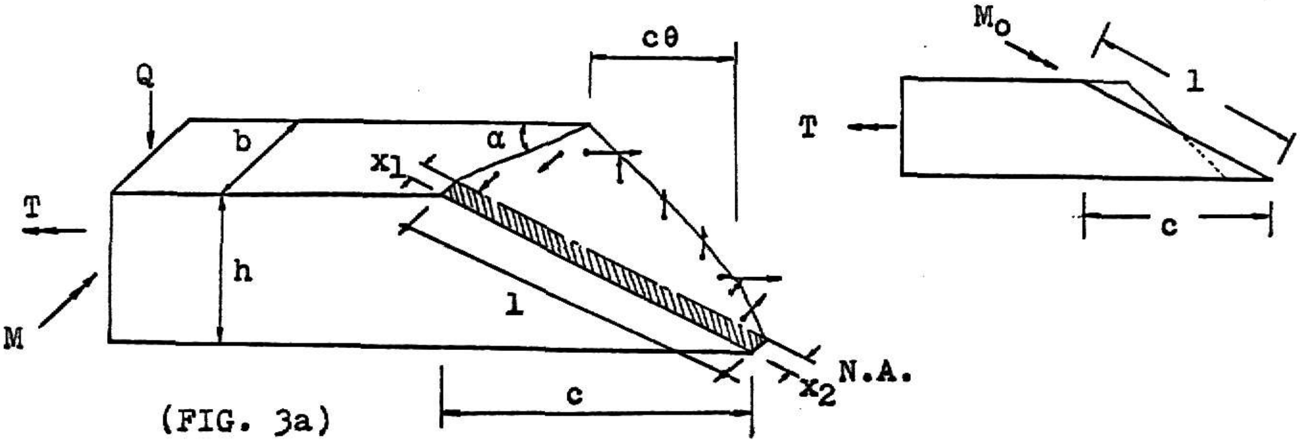


(FIG. 3a)

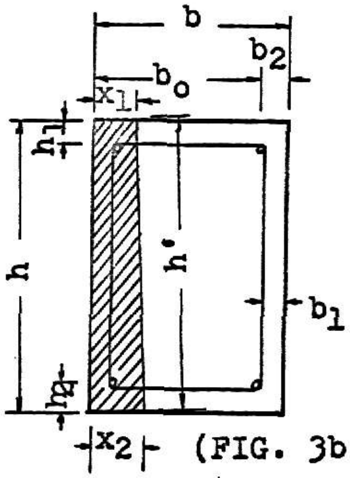


(FIG. 3b)

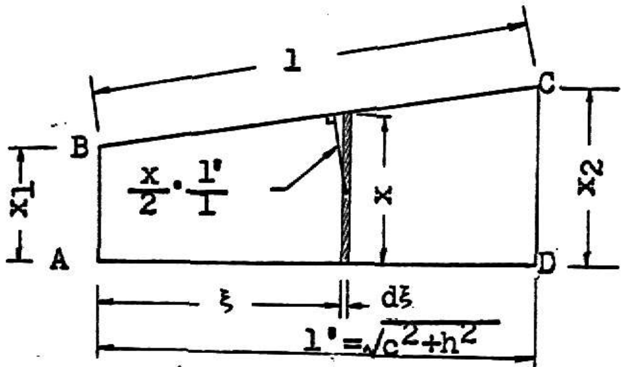


(FIG. 3c)

**FIG. 3 - FREE BODY AND THE FAILURE SURFACE DEFINED BY LESSIG**

B). $M_2$ (due to the longitudinal bars on the right side)

From assumption (1), the total tensile forces act at a point halfway between the two longitudinal bars. Putting $\xi = l'/2$ into (2),

$$x = \frac{x_1 l' + (x_2 - x_1) l'/2}{l'} = (x_1 + x_2)/2$$

and

$$M_2 = f_y \cdot A_s \cdot \left(\frac{h}{h'}\right) \left(b_o - \frac{x_1 + x_2}{2}\right) \left(\frac{h'}{l}\right)$$

$$= f_y \cdot A_s \cdot \left(b_o - \frac{x_1 + x_2}{2}\right) \frac{h}{l} \qquad (4)$$

wherein

$f_y$ - tensile yielding stress of the longitudinal steel.

$A_s$ - area of longitudinal steel on one side of the beam.

h' - the projection of BC(Fig. 3c) on a plane perpendicular to the beam axis.

C). $M_3$ (due to the vertical stirrups).

$$M_3 = f_{vy} \cdot \frac{A_{vs}}{s} (c \cdot \theta) \left(b - b_1 - \frac{x_1 + x_2}{2}\right) \frac{c}{l} \qquad (5)$$

wherein

$f_{vy}$ - tensile yielding stress of the stirrup steel.

$A_{vs}$ - cross-sectional area of one stirrup.

D). $M_4$ (due to the horizontal stirrup of the beam).

Assume the angle between the cracks on both horizontal faces of the beam and the beam axis are the same and let (see Fig.3a)

$$\text{ctn}\ \alpha = \frac{(l - \theta)\ c}{2b - (x_1 + x_2)}$$

then the lever arm of the total stirrup steel on the upper face is

$$\left\{\left[\frac{1}{2} (b - x_1)\ \text{ctn}\ \alpha\right] \frac{h}{c} - h_1\right\} \cdot \frac{c}{l}$$

thus
$$M_4^u = f_{vy} \left[\frac{A_{vs}}{s} (b - x_1)\ \text{ctn}\ \alpha\right] \left[\frac{b - x_1}{2}\ \text{ctn}\alpha\ \frac{h}{c} - h_1\right] \frac{c}{l} \qquad (6)$$

Similarly, the lever arm of the total stirrup steel on the bottom face is

$$\left\{\left[\frac{1}{2}(b-x_2)\ \mathrm{ctn}\ \alpha\right]\frac{h}{c}-h_1\right\}\frac{c}{l} \quad \text{and}$$

$$M_4^b = f_{vy}\left[\frac{A_{vs}}{s}(b-x_2)\ \mathrm{ctn}\ \alpha\right]\left[\frac{b-x_2}{2}\ \mathrm{ctn}\alpha\frac{h}{c}-h_1\right]\frac{c}{l} \quad (7)$$

Combining equation(6) and equation(7) yields

$$M_4 = f_{vy}\frac{A_{vs}}{s}\cdot\frac{c^2}{l}(1-\theta)\left[\frac{h(1-\theta)}{2}\cdot\frac{(b-x_1)^2+(b-x_2)^2}{(2b-x_1-x_2)^2}-h_1\right] \quad (8)$$

Since $M_1$, $M_2$, $M_3$, $M_4$ are all taken about the neutral axis,

$$M_o = M_1 + M_2 + M_3 + M_4$$

and

$$T\cdot\frac{c}{l} = \frac{f_c(c^2+h^2)}{6\ l}(x_1^2+x_1x_2+x_2^2)$$

$$+ f_y A_s'\left(b_o-\frac{x_1+x_2}{2}\right)\frac{h}{l}$$

$$+ f_{vy}\cdot\frac{A_{vs}}{s}\cdot\frac{c^2}{l}\left(b-b_1-\frac{x_1+x_2}{2}\right)$$

$$+ f_{vy}\frac{A_{vs}}{s}\cdot\frac{c^2}{l}(1-\theta)\left[\frac{h(1-\theta)}{2}\cdot\frac{(b-x_1)^2+(b-x_2)^2}{(2b-x_1-x_2)^2}-h_1\right] \quad (9)$$

In equation(9), the internal moment is a function of four parameters - $x_1$, $x_2$, c and $\theta$. For a certain value of c and $\theta$, a change in either $x_1$ or $x_2$ will change the value of internal resisting moment. Recognizing that the beam would fail in such a state that the location of the neutral axis corresponds to the minimum internal moment, equation(9) is differentiated with respect to $x_1$ and $x_2$. This procedure yields the result that $x_1 = x_2$. As a consequence, equation(9) can be written:

$$T \cdot c = \frac{f_c\ (c^2 + h^2)}{2} x^2 + A_s\ f_y\ (b_o - x)\ h$$

$$+ f_{vy} \frac{A_{vs}}{s} c^2 \left\{ \theta(b - b_1 - x) + (1-\theta)\left[\frac{h(1-\theta)}{4} - h_1\right]\right\} \qquad (10)$$

$$f_c \cdot (c^2 + h^2)x - A_s \cdot f_y \cdot h - \frac{A_{vs}\ f_{vy}}{s} \cdot c^2\theta = 0 \qquad (11)$$

Equation(11) is obtained by differentiating equation(10) with respect to x. This equation indicates the equilibrium of the projections of all forces acting normal to the plane of the compression zone. Solving for x yields

$$x = \frac{A_s\ f_y\ h + A_{vs}\ f_{vy}\ c^2\theta / s}{f_c\ (c^2 + h^2)} \qquad (12)$$

Multiplying equation(11) by x/2 and subtracting from equation(10),

$$T \cdot c = A_s \cdot f_y(b_o - \frac{x}{2})\ h - f_{vy}\frac{A_{vs}}{s} c^2 \left\{ \theta(b - b_1 - \frac{x}{2}) \right.$$

$$\left. + (1 - \theta)\left[\frac{h\ (1-\theta)}{4} - h_1\right]\right\} \qquad (13)$$

If the following expressions are introduced,

$$p = \frac{f_{vy} \cdot A_{vs} \cdot b}{f_y \cdot A_s \cdot s}$$

$$z = b_o - x/2 \qquad (14)$$

$$y = \theta(b - b_1 - \frac{x}{2}) + (1-\theta)[\frac{h(1-\theta)}{4} - h_1]$$

equation (13) can be simplified as

$$T = A_s \cdot f_y \cdot \frac{z + pc^2 y/bh}{c/h} \tag{15}$$

The value of c corresponding to the minimum value of beam resistance can be obtained by differentiating equation (14) partially with respect to c. The result is

$$c = \sqrt{z \cdot b \cdot h \; / \; p \cdot y} \tag{16}$$

In many cases, c obtained from equation (16) is larger than the actual values of c measured in tests. This is because of the effect of the concrete in tension. Lessig suggested that

$$c_{max} \leq 2b + h$$

Due to the fact that the transverse reinforcement is not uniformly distributed and the cross-sectional area of the stirrups intersecting the surface of failure could be less than that assumed in deriving the design equations, a correction should be applied to the value of y in equation (14) as following,

$$y = (\theta - \frac{s}{c})(b - b_1 - \frac{x}{2}) + \frac{h}{4}(1 - \theta - \frac{2s}{c})(1 - \theta - \frac{4h_1}{h}) \tag{17}$$

In order to simplify computation, a correction coefficient of 0.7 to 0.8 is generally applied to p instead of using equation (17). This coefficient takes into account the reduction in the actual cross-sectional area of the stirrups that intersect the surface of failure.

To compute the ultimate torque in a test, the actual value of c and $\theta$ can be measured. However, there is no such information available when designing a beam. Thus an approximation of $\theta$ with sufficient accuracy for practical purposes was proposed by Lessig based on her experience.

$$\theta \cong h \,/\, (2b + h) \tag{18}$$

Equation (18) is reasonably good for pure torsion, since the cracks of concrete start before stress redistribution and the principal tensile stresses at this stage always have an angle of $45^{o}$ to the beam axis.

If the principal tensile stresses in torsion are constant over the entire cross-section and equal to the ultimate tensile strength of the concrete, the twisting moment that produces the formation of cracks is determined by the plasticity equation

$$T = f_t \frac{b^2}{6}(3h - b) \tag{19}$$

Starting from equation (18), and letting $z/y = 1/\theta$, the value of c in equation (16) can be calculated. Substituting this value into equation (12), the ultimate torque T as well as values of z and y can be obtained by using equations (14) and (15). For a more accurate solution, a second computation can be carried out by putting the value of z and y that are thus obtained into equation (16) and repeating the same procedures as before.

It is necessary to point out that the design equations derived in this section are on the basis of some assumptions. Thus, these equations are valid only when failure starts with yielding of the reinforcement. And at the present stage, to the best of our knowledge, the ultimate load-bearing capacity of a reinforced concrete beam that fails through the failure of the concrete is still unknown. Lessig suggested (6) an empirical equation for calculating the ultimate torsional moment in case that the beam is over-reinforced.

$$M_k = k \cdot f_c' \cdot b^2 \cdot h \tag{20}$$

The coefficient k in equation (20) must be obtained from experimental data. A value of 0.07 is considered to be on the safe side.

However, it is preferred to have beams which are not over-reinforced. Theoretically there exists a ratio of transverse to longitudinal steel which guarantees that the steel in both directions will reach the yield stress before there is inadmissible deformation or objectional cracking during the stress redistribution in the steel. For a beam loaded in pure torsion, the optimum value of p(in equation 14) under which yielding of reinforcement occurs simultaneously in all tension bars crossing the crack was given by Lessig as 1.0. Empirical data, however, confirm that any value between 0.5 and 1.5 is applicable without producing complications in practical design.

## HSU'S THEORY FOR PURE TORQUE

A series of 53 beams loaded in pure torsion was tested by Hsu, beginning in 1962. After study of these test results and the results reported by others, Hsu pointed out (11) that Lessig's theory overestimates the torsional resistance of a beam and that her theory does not agree with the following observed phenomena:

1). The horizontal stirrups usually have small tensile stresses when the failure machanism forms. Occasionally, these horizontal legs are in compression. Lessig assumed that they were in tension and that they all reach the yield point.

2). Diagonal cracks on the wider face of the beam extend perpendicular to the corner into the shorter face. The angle of the cracks on the shorter faces is frequently much less than 45 degrees.

3). The dowel action which exists in the longitudinal steel was not considered in Lessig's theory. This action was confirmed, by Hsu, by measuring the bending stresses from diametrically opposite sides of a longitudinal corner bar.

4). At ultimate torque, the cracks at the corners and on the shorter faces are wider than those at the center of the wider faces. This indicates that the neutral axis about which the free body rotates is different from what Lessig assumed.

In 1968, Hsu presented a new approach to the analysis of a reinforced concrete beam subjected to torsion. His theory involves the assumption of a new surface of failure which is compatible with his experimental observations. To study Hsu's theory, both the behavior of plain concrete beams and reinforced concrete beams must be considered.

I. Plain Concrete Rectangular Beams

According to Hsu's paper (9), the surface of failure for a plain concrete rectangular beam as found in tests is shown in Fig. 4. Instead of a spiral form, the crack starts from the middle of one wider face and extends into the two shorter faces almost perpendicualr to the corner then turns gradually toward 45 degrees as it approaches the opposite wider face. The cracks on the wider faces are at approximately 45 degrees to the edges of the face and the failure surface is approximately a plane. Furthermore, the concrete near the face where the cracks begin seems to fail in tension but the concrete near the other face seems to be in compression. These observations indicate that a concrete beam subjected to pure torsion fails by bending action on a plane which is normal to both the wider faces and inclined at an angle of $\phi$ to the beam axis. (See Fig. 5)

The equilibrium equation about the neutral axis can be set up as

$$M_o = T_{up} \cdot \cos \Phi \qquad (21)$$

This equation can be simplified through the use of the concept of the modulus of rupture, $f_r$, which is defined as the value of f calculated by using the flexure equation $f = M \cdot y/I$, when M is the maximum bending moment in a beam loaded to rupture.

Using the flexure equation and the above definition of the modulus of rupture we obtain

$$M_o = \frac{b^2\ h}{6} \cdot \csc\phi \cdot f_r \qquad (22)$$

wherein, $M_o$ - moment about the neutral axis.

$T_{up}$ - ultimate torque applied to the plain concrete rectangular beam.

$\phi$ - angle between the assumed failure surface and the beam axis.

$f_r$ - modulus of rupture of concrete.

combining equation (21) and (22) yields

$$T_{up} = \frac{b^2\ h}{6} \cdot f_r \cdot (\sec\phi\ \csc\phi) \qquad (23)$$

Equation (23) yields the torsional resistance of a beam which varies as a function of the parameter $\phi$. The value of $\phi$ corresponding to the minumum strength of the beam can be found by differentiating this equation with respect to $\phi$ and setting the differentiated equation equal to zero. This yields the result, $\phi = 45^o$.

Consequently,

$$T_{up} = b^2 \cdot h \cdot f_r\ /\ 3 \qquad (24)$$

The value of $f_r$ in equation (24) is obtained by a flexure test. It should be reduced, according to Mohr's theory, in case that perpendicular compression exists. Since perpendicular compression does not exist in the flexure test but always

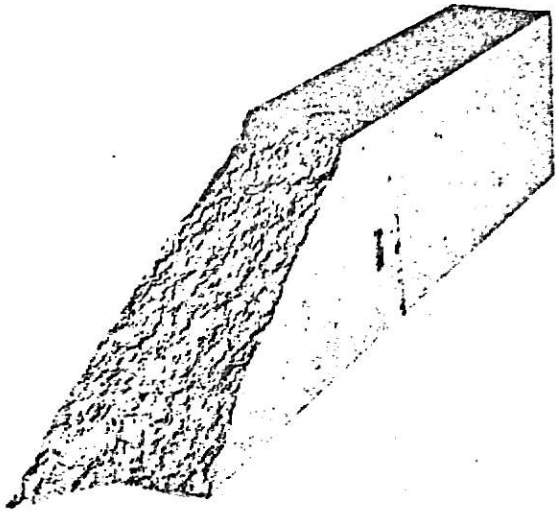

FIG. 4 - FAILURE SURFACE OF 10x15-in. BEAM(A1)
IN HSU'S TESTS

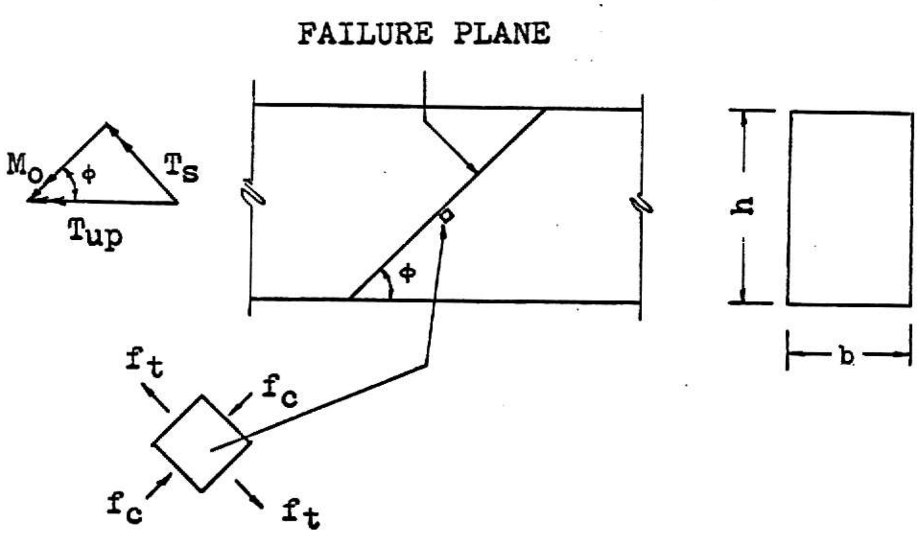


FIG. 5 - COMPONENTS OF APPLIED TORQUE AND
STRESSES ON ELEMENT IN FACE OF BEAM

exists in torsion, Hsu applied a reduction factor equal to 0.85 to $f_r$. This factor was obtained from experimental data. Thus, equation (24) is written in the form

$$T_{up} = b^2 \cdot h \cdot (0.85\ f_r)/3. \tag{25}$$

A comparison of the results calculated using equation (25) and the test results is shown in Table I-1, Appendix I. It can be seen that the values obtained by this equation are reasonably close, within 6 percent, to the test results.

For practical purposes, it is more advantageous to use the tensile or compressive strength of concrete rather than the modulus of rupture. If the relationship between them can be found, equation (25) can be transformed into a more suitable form for design purposes. To establish such a relationship, the tensile strength of concrete, $f_t$, is considered first.

Let $\quad f_r = K \cdot f_t$

Here K is a coefficient which is influenced by many factors. But of all these factors, the size of the beam and the tensile strength of the concrete will predominate in determining the magnitude of this coefficient. The influences of these two factors are found from the test results and reported by Hsu (9). For beams having depths larger than 4 inches, the value of K is as follows:

$$K = \frac{7.17}{\sqrt[3]{f_t}} \left(1 + \frac{10}{b^2}\right) \tag{26}'$$

and equation (25) becomes

$$T_{up} = 2\ (b^2 + 10) \cdot h\ \sqrt[3]{f_t^2} \tag{26}$$

For beams having depths between 2 inches and 4 inches, a different value was obtained.

$$K = \frac{7.17}{\sqrt[3]{f_t}} \cdot \frac{2.4}{\sqrt[3]{b}} \tag{27'}$$

$$T_{up} = 4.9\ \sqrt[3]{b^5} \cdot h\ \sqrt[3]{f_t^2} \tag{27}$$

The relationship between tensile strength, $f_t$, and compressive strength, $f'_c$, depends on age, water-cement ratio, mix proportion, moisture content, etc. But generally, it can be expressed as

$$f_t = 5 \cdot \sqrt{f'_c} \tag{28}$$

Using this expression, equations (26) and (27) are transformed into a form based on $f'_c$. Equation (26) yields

$$T_{up} = 6\ (b^2 + 10)\ h\ \sqrt[3]{f'_c} \tag{29}$$

and equation (27) yields

$$T_{up} = 14.3\ \sqrt[3]{b^5}\ \ h\ \sqrt[3]{f'_c} \tag{30}$$

Equations (29) and (30) are equations for calculating the ultimate resistance of a plain concrete rectangular beam. A comparison of the values calculated from equation (29) and experimental results was made by Hsu in his paper (9). Equation (29) appears to be acceptable. Eqaution (30) is to be used primarily for model tests. However, Hsu did not check the validity of this equation.

II. Reinforced Concrete Rectangular Beams

For a reinforced concrete rectangular beam subjected to pure torque, the behavior before the concrete cracks is quite different from the behavior after the concrete cracks. It has been shown in experiments (10) that before cracking, the beam will behave just like a plain concrete beam. However, there are some stresses in the steel prior to cracking, and the torque which causes cracking will increase as the amount of steel reinforcement increases. The relationship is

$$T_{cr} = (1.0 + 0.04\ p_t) \cdot T_{up}$$

in which, $T_{cr}$ - the quantity of torque when beam cracking was first seen on the concrete surface.

$p_t$ - the percentage of total steel by volume in the concrete beam.

$T_{up}$ - the ultimate resistance of a plain concrete rectangular beam of the same size.

As soon as the concrete cracks, the angle of twist of the beam will continue to increase under a constant torque until a new state of equilibrium is generated, and the stresses in the reinforcement increase suddenly during this stage. This new type of equilibrium after cracking is considered to be an equilibrium of moments as well as forces in a plane, the failure plane, which is perpendicular to two vertical faces and has an angle of 45° to the beam axis (Fig. 6). In other words, the failure surface of a reinforced concrete beam is identical to that of a plain concrete beam. The reason for this is that the reinforcement has only a small effect before the beam cracks. After cracking, the surface of failure will not be significantly changed although the reinforcement then begins to carry the tensile forces. For this reason, the neutral axis is a straight line in the failure plane and is parallel to the vertical faces of the beam. The compression zone, which is also subjected to shear, is shown as the shaded area in Fig. 6.

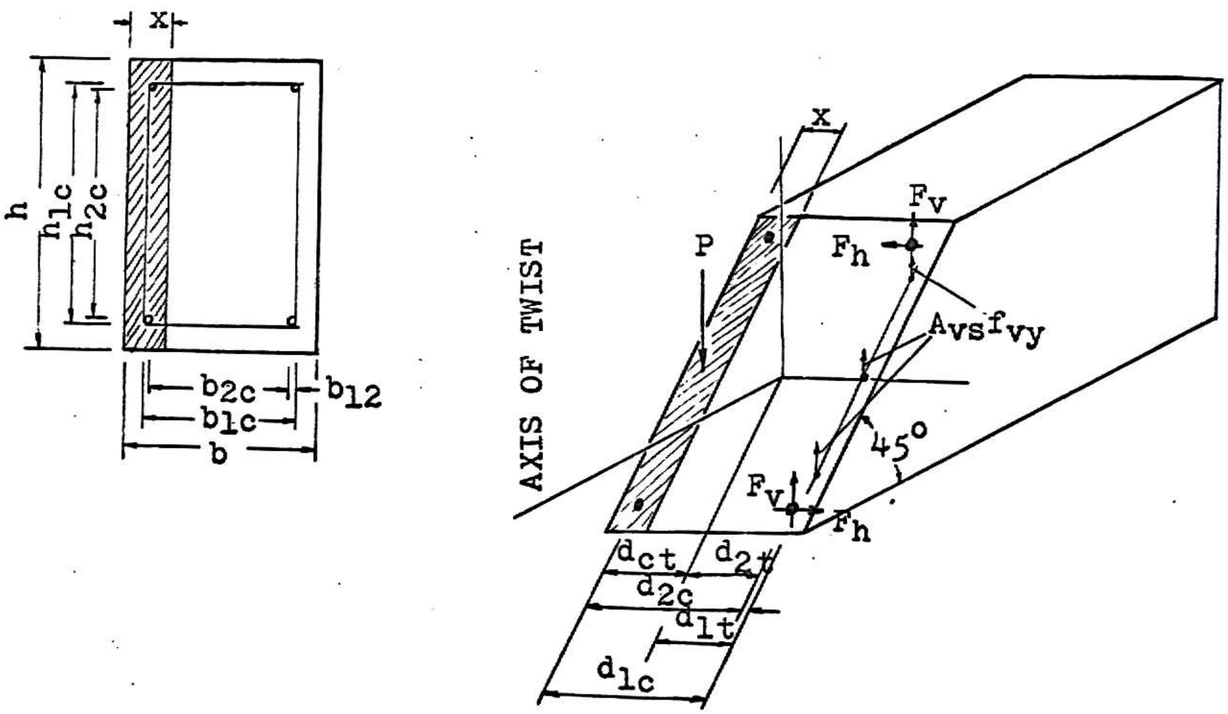


FIG. 6. - FAILURE SURFACE AND CROSS SECTION PROPOSED BY HSU

Since the surface of failure as well as the failure mode has been determined, the design equation can be derived from the equilibrium equations of the free body. Refering to Fig. 6, the resisting moment of the beam about the axis of twist is made up of several parts - the tensile forces in the steel reinforcement, the compression in the concrete, and the dowel forces in the steel reinforcement. As mentioned before, the forces contributed by the horizontal stirrups are excluded in Hsu's theory because during the tests they appeared to be small, irregular, and at least part of the time were compressive forces. On the other hand, the dowel forces which are not considered in Lessig's theory will be considered here.

The resisting moment contributed by the vertical stirrups is

$$M_{vs} = \frac{h_{1c}}{s} \cdot A_{vs} \cdot f_{vy} \cdot d_{1t} \qquad (31)$$

wherein, $M_{vs}$ - moment about the axis of twist due to the vertical stirrups that intersect the surface of failure in the tensile zone.

$h_{1c}$ - larger center-to-center dimension of a closed rectangular stirrup.

$d_{1t}$ - distance from the center of the vertical stirrups in the tensile zone to the axis of twist.

The resisting moment contributed by the horizontal dowel forces of the longitudinal steel is

$$M_{fh} = 2\ F_h \cdot \frac{h_{2c}}{2} = F_h \cdot h_{2c} \qquad (32)$$

wherein, $F_h$ - horizontal dowel force of one longitudinal bar in the tensile zone.

$h_{2c}$ - vertical center-to-center distance of the longitudinal corner bars.

The resisting moment contributed by the vertical dowel forces in the longitudinal steel is

$$M_{fv} = 2\ F_v \cdot d_{2t} \tag{33}$$

wherein, $F_v$ - vertical dowel force in one logitudinal bar in the tensile zone.

$d_{2t}$ - horizontal distance between the center of the longitudinal bars in the tensile zone and the axis of twist.

So far, we have not considered the forces acting in the direction of the beam axis. In the vertical direction, the concrete compression, concrete shear and tensile force in the longitudinal bars in the shear-compression zone must combine to yield a vertical force which is in equilibrium with the sum of the vertical dowel forces and the tensile stirrup forces. Let this vertical force be P, then

$$P = \frac{h_{1c}}{s} A_{vs} \cdot f_{vy} + 2\ F_v \tag{34}$$

The magnitude of P can be determined from the force polygon shown in Fig. 7. There are three known forces in the polygon, the shear force in the concrete, $P_s$, the compressive force in the concrete, $P_c$, and the horizontal force in the longitudinal steel, $P_l$. From the geometry

$$P = \sqrt{2}\ P_s + P_l \tag{35'}$$

For under-reinforced beams, the steel reaches its yield stress before the concrete crushes.

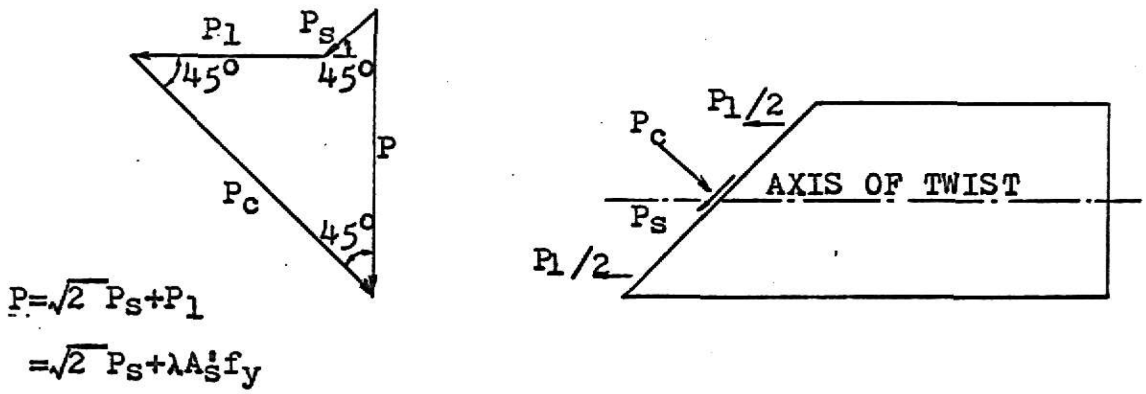


FIG. 7 - THE FORCE POLYGON IN THE SHEAR-COMPRESSION ZONE

Thus, equation (35)' can be transformed to

$$P = \sqrt{2} \cdot P_s + \lambda A_s' f_y \tag{35}$$

wherein, $A_s'$ - cross-sectional area of longitudinal bars within the shear compression zone. Generally, it is equal to one-half of the total longitudinal steel area and is therefore equal to $A_s$.

$\lambda$ - an efficiency coefficient introduced because the longitudinal steel is not uniformly distributed over the shear-compression zone and should not be considered fully effective.

The moment contributed by this force is the product of this force times its lever arm.

$$M_c = (\sqrt{2}\ P_s + \lambda A_s' f_y)\ d_{ct} \tag{36}$$

in which, $d_{ct}$ - the distance from the center of the shear-compression zone to the axis of twist.

The total resisting moment is obtained by summing equations (31), (32), (33), and (36).

$$T_u = \sqrt{2}\ P_s \cdot d_{ct} + \lambda A_s' \cdot f_y \cdot d_{ct} + \frac{h_{1c}}{s} A_{vs} \cdot f_{vy} \cdot d_{1t}$$

$$+ F_h\ h_{2c} + 2\ F_v\ d_{2t} \tag{37}$$

Equations (34) and (35) are combined to obtain

$$\frac{h_{1c}}{s} A_{vs}\ f_{vy} + 2\ F_v = \sqrt{2}\ P_s + \lambda A_s'\ f_y \tag{38}$$

Equations (37) and (38) represent equilibrium of the moments about the axis of twist and the forces in the vertical direction respectively. By using equation (38), the vertical dowel force $F_v$ in equation (37) can be eliminated. In addition, some algebraic work will bring equation (37) to a simpler form,

$$T_u = \sqrt{2}\ P_s \cdot d_{2c} + \left[\frac{b_{12}}{b_{1c}} + \lambda m \frac{f_y}{f_{vy}} \left(1 + \frac{b_{1c}}{h_{1c}}\right) \frac{d_{2c}}{b_{1c}}\right]$$

$$\times \frac{b_{1c}\ h_{1c}\ A_{vs}\ f_{vy}}{s} + F_h\ h_{2c} \tag{39}$$

wherein, $d_{2c}$ - the distance from the center of the longitudinal steel to the center of the compression zone (equal to the sum of $d_{2t}$ and $d_{ct}$).

$b_{12}$ - the distance from the center of the stirrup to the center of the nearest longitudinal bar (equal to the sum of the radius of the longitudinal bar and the radius of stirrup).

$b_{1c}$ - small center-to-center dimension of a closed rectangular stirrup.

m - ratio of the volume of longitudinal bars to the volume of stirrups, i.e., $m = A_s \cdot s / [A_{vs} \cdot (b_{1c} + h_{1c})]$.

To find the horizontal dowel force in the longitudinal steel, two assumptions must be made which are based on experimental observations. These two assumptions are

a). the dowel force is proportional to the cross-sectional area of the bars.

b). the dowel force is proportional to the relative lateral displacement of the bars across the failure surface.

Then the equation for the horizontal dowel force is

$$F_h = q \cdot (A_s/2) \cdot \bar{\theta} \cdot (h_{2c}/2) \qquad (40)$$

wherein, q - dowel stresses per unit displacement, in in-lb per cu.in., a constant.

$\bar{\theta}$ - relative angle of twist of the two surfaces of the failure crack, in radians, roughly a constant.

Substituting, $2 \cdot A_s = m \cdot A_{vs} \cdot (b_{1c} + h_{1c})/s$, into equation (40), rearranging it and multiplying both side by $h_{2c}$ yields

$$F_h\, h_{2c} = \left[\frac{1}{4}\cdot\frac{q\cdot\bar{\theta}}{f_{vy}}\cdot\frac{h_{2c}^2}{h_{1c}}\cdot\left(1 + \frac{h_{1c}}{b_{1c}}\right)m\right]\frac{b_{1c}h_{1c}A_{vs}f_{vy}}{s} \qquad (41)$$

The dowel action is still not well understood. Tests have revealed that the dowel stress is affected by the spacing of the stirrups too. However, for stirrup spacing smaller than $0.5h_{1c}$, the effect of spacing is not large and can apparently be neglected.

Substituting equation (41) into equation (39) results in the following:

$$T_u = \sqrt{2}\, P_s\, d_{2c} + \left[\frac{b_{12}}{b_{1c}} + \lambda m \frac{f_y}{f_{vy}}\left(1 + \frac{b_{1c}}{h_{1c}}\right)\frac{d_{2c}}{b_{1c}} + \frac{1}{4}\left(\frac{q\cdot\bar{\theta}}{f_{vy}}\right)\frac{h_{2c}^2}{h_{1c}}\left(1 + \frac{h_{1c}}{b_{1c}}\right) m\right] \frac{b_{1c}h_{1c}A_{vs}f_{vy}}{s} \qquad (42)$$

In order to simplify equation (42), two identities can be introduced.

$$T' = \sqrt{2}\, P_s\cdot d_{2c}$$

and

$$K' = \frac{b_{12}}{b_{1c}} + \lambda m\, \frac{f_y}{f_{vy}}\left(1 + \frac{b_{1c}}{h_{1c}}\right)\frac{d_{2c}}{b_{1c}} + \frac{1}{4}\left(\frac{q\cdot\bar{\theta}}{f_{vy}}\right)\frac{h_{2c}^2}{h_{1c}}\left(1 + \frac{h_{1c}}{b_{1c}}\right) m \qquad (43)$$

Equation (42) then becomes

$$T_u = T' + K'\, b_{1c}\, h_{1c}\, \frac{A_{vs}\, f_{vy}}{s} \qquad (44)$$

Equation (44) is in the same form as the ultimate design equations for pure torque in the 1958 German Code and the 1958 Australian Code. However it is inconvenient to use this equation to predict the ultimate torsional resistance of a beam since we have not determined values of T' and K'. Further discussion of this equation is necessary. The discussion will be divided into two parts, one concerning T' and the other concerning K'.

A). T' - the resisting torque provided by the shear strength of the concrete in the shear-compression zone.

If the effect of stirrups within this region is neglected, and the average shear stress is denoted by $v_{av}$

then

$$P_s = v_{av} \cdot \sqrt{2}\, h \cdot x \tag{45}$$

the values of $v_{av}$ and x can be expressed as

$$v_{av} = k_1 \cdot v'_c. \qquad\qquad x = k_2 \cdot b$$

in which $k_1$ and $k_2$ are undetermined coefficients. Now

$$P_s = \sqrt{2}\, k_1 \cdot k_2 \cdot b \cdot h \cdot v'_c \tag{46}$$

To transform $v'_c$ in equation (46) in terms of $f'_c$, the relationship $v'_c = [f'_c / (f'_c + f_t)]f_t$ is used (13). Hsu suggested a value of 0.9 for the terms in the parenthesis, $[f'_c / (f'_c + f_t)]$, since the uniaxial tensile strength, $f_t$, is rather small in comparison to the cylinder compressive strength. As stated before on page 19, $f_t = 5\sqrt{f'_c}$.

Thus,

$$P_s = 6.4 \cdot k_1 \cdot k_2 \cdot b \cdot h \cdot \sqrt{f'_c} \tag{47}$$

Substituting equation (47) into equation (43) and assuming $d_{2c} = 0.8b$,

$$T' = 7.2 \cdot k_1 \cdot k_2 \cdot b^2 \cdot h\, \sqrt{f'_c} \tag{48}$$

It is difficult to evaluate $k_1$ and $k_2$, because of insufficient information. However, it can be shown that $T'$ is approximately a constant (11) and roughly equal to the value $T_o$ (See Fig. 8) which is obtained experimentally as the intercept of a test curve with the $T_u$ axis. The value of $T_o$ was found by Hsu from his experimental data as

$$T_o = \frac{2.4}{\sqrt{b}} \cdot b^2 \cdot h \cdot \sqrt{f'_c} \qquad (49)$$

As shown in Fig. 8, the terms $T'$ and $T_o$ have different meanings. However, for the purpose of design, these two can be set equal.

Then $\quad k_1 \; k_2 = 0.33 \; / \sqrt{b}$

and $$T' = \frac{2.4}{b} \, b^2 \; h \sqrt{f'_c} \qquad (50)$$

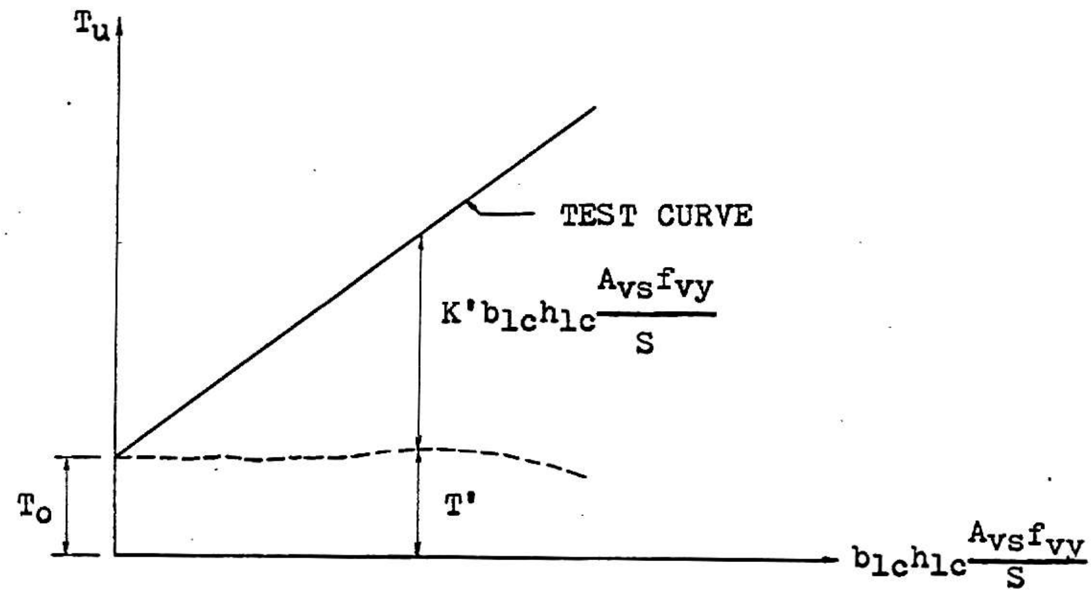


FIG. 8 - THE RELATIONSHIP BETWEEN $T_o$ AND $T'$

A comparison of the values obtained using equation (50) and test results was done by Hsu (11). This comparison is copied in Table I-2, Appendix I, which shows that they compare favorably with each other.

B). K' - the coefficient in the second term.

The value of K' should be evaluated from equation (43). However, there are three coefficients, $\lambda$, q and $\bar{\theta}$, which are not available because a reasonable analysis for them has not been established. Due to this fact, Hsu used experimental data to evaluate K' rather than determining it theoretically.

By carefully studying the relationships of K' versus m, $f_y / f_{vy}$, $h_{1c} / b_{1c}$ and $h_{2c}$, it can be seen that the effect of $h_{2c}$ can be neglected due to its small effect. Furthermore, if $f_y = f_{vy}$ and assuming K' is a function of these factors to the first power, then the value of K' is

$$K' = j_1 + j_2 \cdot m + j_3 \cdot h_{1c} / b_{1c} \tag{51}$$

The coefficients $j_1$, $j_2$ and $j_3$ have to be evaluated from experimental results. For the case when m = 1.0, $f_y = f_{vy}$, $h_{1c} / b_{1c} \leq 2.6$,

Hsu found

$$K' = 0.66 + 0.33 \frac{h_{1c}}{b_{1c}} \tag{52}$$

Equating equations (51) and (52) gives

$$j_1 + j_2 = 0.66 \qquad \text{and} \qquad j_3 = 0.33$$

Further investigation shows $j_1$ can reasonably be taken as 0, so

$$K' = 0.66\ m + 0.33\ \frac{h_{1c}}{b_{1c}} \tag{53}$$

In case $f_y \neq f_{vy}$, the value of K' should be

$$K' = 0.66 \cdot m\ \frac{f_y}{f_{vy}} + 0.33\ \frac{h_{1c}}{b_{1c}} \tag{54}$$

Combining equations (44), (50) and (54) gives the design equation for a reinforced concrete rectangular beam in pure torque.

$$T_u = \frac{2.4}{\sqrt{b}}\ b^2 h \sqrt{f'_c} + \left(0.66\ m \frac{f_y}{f_{vy}} + 0.33 \frac{h_{1c}}{b_{1c}}\right) \frac{b_{1c} h_{1c} A_{vs} f_{vy}}{s} \tag{55}$$

Equation (55) is the design equation obtained by using equation (44) and the experimental data. According to Hsu's tests, this equation should be checked against the following limitations in order to assure its validity.

a. If $h_{1c}/b_{1c} > 2.6$, a value of 2.6 should be used in equation (54). Consequently,

$$T_u = \frac{2.4}{\sqrt{b}}\ b^2 h \sqrt{f'_c} + \left(0.66\, m\, \frac{f_y}{f_{vy}} + 0.858\right) \frac{b_{1c} h_{1c} A_{vs} f_{vy}}{s} \tag{56}$$

b. The total reinforcement provided must be less than the balanced total volume percentage, $P_{tb}$. This limitation assures that the beam will not fail through the crushing of the concrete. An empirical equation for $P_{tb}$ as found by Hsu is (10).

$$P_{tb} = 2400\ \frac{\sqrt{f'_c}}{f_{vy}} \tag{57}$$

As a matter of fact, $P_{th}$ is affected by m and $h_{1c}/b_{1c}$ too. But these effects are neglected due to insufficient data and also because they appear to be small in comparison with the effects of $f'_c$ and $f_{vy}$.

If the total reinforcement is larger than $P_{th}$, the total percentage of steel is to be taken as $2400 \sqrt{f'_c} / f_{vy}$ while maintaining the same $m\ f_y/f_{vy}$ ratio.

c. The full utilization of the reinforcement is affected by the ratio of the volume of longitudinal steel to the volume of stirrup steel, m. For a small percentage of reinforcement, m could have a large permissible variation. But for a high percentage of reinforcement, the beam is very sensitive to the variation of m. To assure the full utilization of reinforcement, the value of $m \cdot f_y/f_{vy}$ can not be larger than 1.5 or smaller than 0.7. If $m \cdot f_y/f_{vy} > 1.5$, the excessive longitudinal steel should be neglected. On the other hand, if $m \cdot f_y/f_{vy} < 0.7$, the excessive percentage of stirrups reinforcement should be neglected.

d. The height-to-width ratio should be equal or larger than 1.5. For smaller ratios, a different type of crack pattern was observed.

e. The spacing of the stirrups has some influence on the ultimate torque of beams. For equal percentages of reinforcement, larger spacing will result in lower resisting torque. Though this influence is not large, it has been proposed to limit the maximum stirrup spacing to $s_{max} = 0.5\ h_{1c}$.

An important phenomenon which appeared in Hsu's tests is that the ultimate torque may not follow the law of similitude (11). Thus the relationship between the model and its prototype in direct model tests may not be considered to be linearly simulated. This phenomenon is still not clear. However, further research in this area is necessary. In this report, a comparison of the results of model tests and Hsu's theory as well as Lessig's theory will be presented.

# REVIEW OF SMALL SCALE MODEL TESTS BY MASON[12]

A). Review of the Experiment

The material used in model tests must be able to simulate the material properties of the prototype. In the test, the substitute for concrete was a mix of 40 percent Ultracal 30, 20 percent Standard Ottowa Sand and 40 percent local crushed limestone between the No. 8 and No. 16 sieves. The weight of water added was 33.3 percent of the weight of the Ultracal 30. The ingredients were mixed with mechanical mixer. Steel forms were used and saturated cloths were placed over the specimens for curing control. All specimens were removed from the forms at the end of the first hour, then covered with saturated cloths for 23 hours. The total curing period was 24 hours and the tests were made on the specimens immediately after the curing period.

The specimens thus obtained were tested for compressive strength and modulus of rupture. The samples cast for these tests were of 1x1x4-in. size. Three batches were tested to determine the uniformity of properties from batch to batch. In each batch, six specimens were tested, three for compression and three for modulus of rupture. The modulus of rupture results were obtained by using a third-point loading test. The results are shown in Table 1.

The relationship between the average value of the compressive strength and the modulus of rupture in each batch can not be checked by the equations established by Hsu (p. 21) since the samples are smaller than 2 inches. However, the compressive strength of the plaster mix simulated that of 3,000 psi. concrete. Although the stress-strain curve showed that the modulus of

TABLE 1

RESULTS FROM COMPRESSION AND MODULUS OF RUPTURE TESTS OBTAINED BY MASON

| | Test Specimen | Batch Number | | |
|---|---|---|---|---|
| | | 1 | 2 | 3 |
| Compressive Strength, in psi. | 1 | 2855 | 3000 | 2710 |
| | 2 | 2690 | 2800 | 2830 |
| | 3 | 2790 | 2845 | 2900 |
| | Average | 2778 | 2882 | 2813 |
| Modulus of Rupture, in psi. | 1 | 414 | 427 | 402 |
| | 2 | 439 | 377 | 389 |
| | 3 | 389 | 452 | 439 |
| | Average | 414 | 419 | 410 |

elasticity of the Ultracal mix was different from that of the concrete(12), this does not affect the ultimate torsional resistance of the beams.

The element used to simulate the longitudinal bar was a

#6-32 threaded rod, that is, a rod with a #6 nominal diameter and having 32 threads per inch. The tensile area was computed as 0.0075 sq.in. In order for the rods to exhibit a definite yield point, it was necessary to anneal the rod before using it. Three samples were tested after annealling. The details of the process of annealling as well as the construction of the stress-strain curve were presented by Mason in his thesis(12). Taking the average of the modulus of elasticity and the yield point respectively for the three samples, the idealized stress-strain curve was constructed. It was thus found that for the longitudinal reinforcement

$$f_y = 86{,}000 \text{ psi} \qquad E = 19.0 \times 10^6 \text{ psi}$$

The transverse reinforcement for the 1x2-inch beams was No.15 gage smooth black annealed wire and the transverse reinforcement for the 1.41x2.83-inch beams was No.15 gage smooth bright basic wire. The stress-strain curve for each of these elements was constructed in the same way as for the longitudinal reinforcement. The results are listed in Table 2.

TABLE 2

MECHANICAL PROPERTIES FOR THE TRANSVERSE REINFORCEMENT

| | Yield Stress,psi | Modulus of Elasticity,psi |
|---|---|---|
| Black Annealled Wire (for 1x2-in. beams) | 22,800 | $12.0 \times 10^6$ |
| Bright Basic Wire (for 1.41x2.83-in. beams) | 53,000 | $26.6 \times 10^6$ |

The beams under investigation were of two sizes, 1x2-in. and 1.41x2.83-in. Each size grouping had nine beams in which the longitudinal reinforcement was identical. These beams were designed with three different values of p, 0.4, 0.5 and 0.6. That is, each group of three beams had different amounts of transverse reinforcement. This made a total of 18 beams to be tested as shown in Table 3. The typical cross sections of the beams are shown on Fig. 9.

TABLE 3 DESIGN OF MASON'S TESTS FOR PURE TORQUE

| Cross Section | p | | |
|---|---|---|---|
| | 0.4 | 0.5 | 0.6 |
| | 1 | 1 | 1 |
| 1x2-in. | 2 | 2 | 2 |
| | 3 | 3 | 3 |
| | 1 | 1 | 1 |
| 1.41x2.83-in. | 2 | 2 | 2 |
| | 3 | 3 | 3 |

Four quality control samples were cast for each torsion specimen, two for compression tests and two for flexure tests. The results of the tests are presented in Tables 4 and 5. The beams were numbered in such a way that the first numeral indicates the number in each group, the second indicates the beam

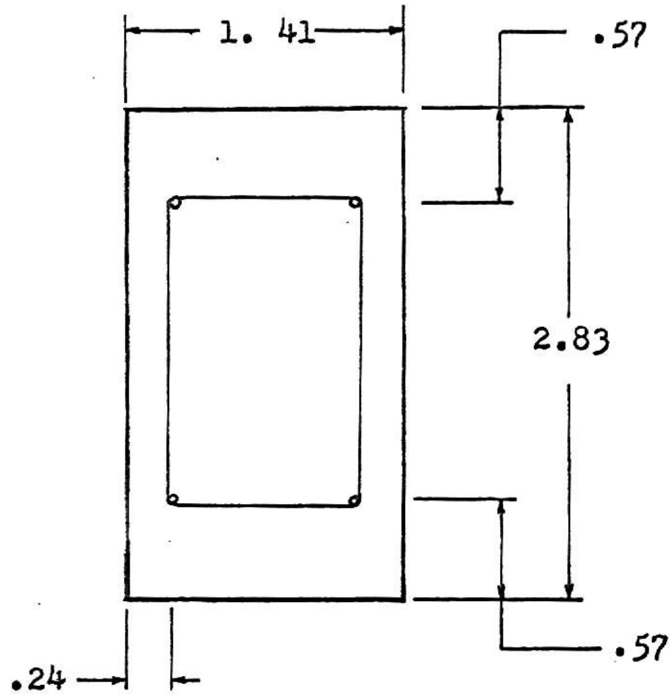


(a) Typical Cross-section of 1.41 x 2.83-in. Beam

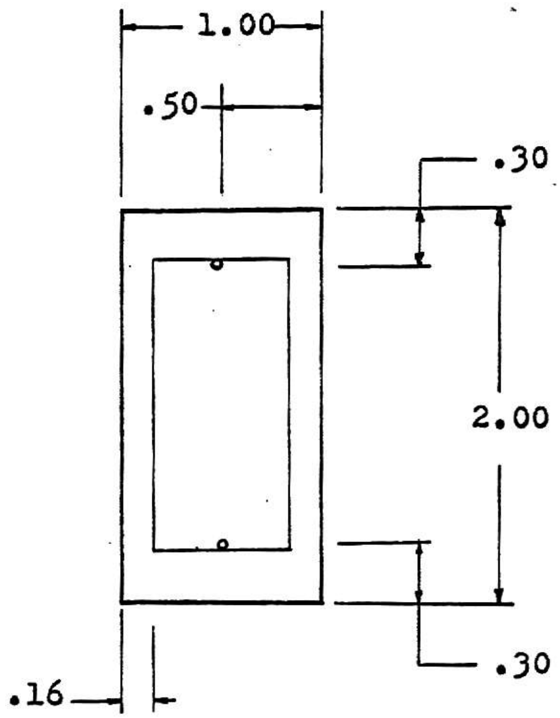


(b) Typical Cross-section of 1 x 2-in. Beam

FIG. 9 - TYPICAL CROSS-SECTION OF TORSION SPECIMENS IN MASON'S MODEL TESTS

TABLE 4

COMPRESSIVE STRENGTH OF QUALITY CONTROL SAMPLES FOR TORSION BEAMS

| | Compressive Strength, psi. | | | | | | | | |
|---|---|---|---|---|---|---|---|---|---|
| Batch | 1 | 2 | 3 | 4 | 5 | 6 | 7 | 8 | 9 |
| Beam | 1-1-.4 | 2-1-.4 | 3-1-.4 | 1-1-.5 | 2-1-.5 | 3-1-.5 | 1-1-.6 | 2-1-.6 | 3-1-.6 |
| (1) | 2,930 | 2,880 | 2,820 | 2,780 | 2,680 | 2,710 | 2,880 | 2,780 | 2,900 |
| (2) | 2,860 | 2,760 | 2,760 | 2,830 | 2,750 | 2,780 | 2,850 | 2,840 | 2,850 |
| Average | 2,895 | 2,820 | 2,790 | 2,805 | 2,715 | 2,745 | 2,865 | 2,810 | 2,875 |
| Batch | 10 | 11 | 12 | 13 | 14 | 15 | 16 | 17 | 18 |
| Beam | 1-1.4-.4 | 2-1.4-.4 | 3-1.4-.4 | 1-1.4-.5 | 2-1.4-.5 | 3-1.4-.5 | 1-1.4-.6 | 2-1.4-.6 | 3-1.4-.6 |
| (1) | 2,840 | 2,810 | 2,760 | 2,860 | 2,820 | 2,790 | 2,750 | 2,800 | 2,830 |
| (2) | 2,790 | 2,880 | 2,810 | 2,790 | 2,900 | 2,720 | 2,840 | 2,720 | 2,770 |
| Average | 2,815 | 2,845 | 2,785 | 2,825 | 2,860 | 2,755 | 2,795 | 2,760 | 2,800 |

Lower Confidence Limit for batch means = 2,709 psi.

Upper Confidence Limit for batch means = 2,907 psi.

TABLE 5

MODULUS OF RUPTURE OF QUALITY CONTROL SAMPLES FOR TORSION BEAMS

| | Modulus of Rupture, psi. | | | | | | | | |
|---|---|---|---|---|---|---|---|---|---|
| Batch | 1 | 2 | 3 | 4 | 5 | 6 | 7 | 8 | 9 |
| Beam | 1-1-.4 | 2-1-.4 | 3-1-.4 | 1-1-.5 | 2-1-.5 | 3-1-.5 | 1-1-.6 | 2-1-.6 | 3-1-.6 |
| (1) | 402 | 414 | 402 | 414 | 452 | 389 | 377 | 402 | 414 |
| (2) | 439 | 377 | 427 | 427 | 414 | 414 | 427 | 439 | 377 |
| Average | 421 | 396 | 415 | 421 | 433 | 402 | 402 | 421 | 396 |
| Batch | 10 | 11 | 12 | 13 | 14 | 15 | 16 | 17 | 18 |
| Beam | 1-1.4-.4 | 2-1.4-.4 | 3-1.4-.4 | 1-1.4-.5 | 2-1.4-.5 | 3-1.4-.5 | 1-1.4-.6 | 2-1.4-.6 | 3-1.4-.6 |
| (1) | 439 | 377 | 427 | 402 | 414 | 452 | 439 | 377 | 439 |
| (2) | 427 | 414 | 389 | 439 | 377 | 414 | 414 | 427 | 389 |
| Average | 433 | 396 | 407 | 421 | 396 | 433 | 427 | 402 | 414 |

Lower Confidence Limit for batch means = 386 psi.

Upper Confidence Limit for batch means = 444 psi.

width and the third indicates the value of p. The upper and lower strength for individual batch means are shown at the bottom of the tables. It can be seen that the average strength of each individual batch falls within these ranges.

The torque was applied concentrically, to the beam tested, through a 20 in. lever arm by a hydraulic jack. The load cell was attached to the lever arm and the force from the jack was applied through the load cell. The cell was designed for a maximum reading of 50,000 lbs. and Mason pointed out that some difficulties were encountered with the accuracy of the load readings since the loads being read were less than 100 lbs. However, the ultimate load cell readings which were obtained are tabulated in Table 6. The average load cell reading, standard deviation and coefficient of variation for each combination of the cross-sectional area and p are also given in this table. Table 7 was prepared by taking some data from Mason's work, such as the actual failure torque and the calculated torque. To allow a comparison of those values against the theoretical results, the ultimate resistances predicted by Lessig's theory are presented in this table too. The computation of the theoretical values is shown in Appendix II. In Table 7,

$T_{actu}$ - actual failure torque determined from load cell readings, in in-lbs.

$T_{calc}$ - ultimate torque calculated by Lessig's theory using the measured parameters, in in-lbs.

TABLE 6

ANALYSIS OF ULTIMATE LOAD CELL READING OF TORSION BEAMS

| Cross Section | p = 0.4 | p = 0.5 | p = 0.6 |
|---|---|---|---|
| | Ultimate Load Cell Readings | | |
| 1 x 2-in. | 32 | 32* | 24* |
| | 24* | 30 | 30 |
| | 37* | 33* | 39 |
| Average | 31 | 32 | 31 |
| Standard Deviation | 6.56 | 2.24 | 7.55 |
| Coefficient of Variation | 21.20 | 1.58 | 24.35 |
| 1.41 x 2.83-in. | 34 | 44 | 46* |
| | 44 | 42* | 47 |
| | 44 | 39* | 40* |
| Average | 41 | 42 | 44 |
| Standard Deviation | 5.79 | 2.55 | 3.81 |
| Coefficient of Variation | 14.24 | 6.12 | 8.59 |

* Measured value of c obtained by adding twice the horizontal projection of the bottom crack to cθ. (See Reference 12).

TABLE 7

MEASURED PARAMETERS AND CALCULATED TORQUE FOR TORSION SPECIMENS

| Beam No. | p | Measured c in. | Measured cθ in. | θ | $T_{actu}$ in-lbs | $T_{calc}$ in-lbs | $T_{theo}$ in-lbs | $T_{actu}/T_{calc}$ | $T_{actu}/T_{theo}$ | $T_{calc}/T_{theo}$ |
|---|---|---|---|---|---|---|---|---|---|---|
| 1-1-0.4 | 0.40 | 3.69 | 2.19 | 0.594 | 640 | 494 | 884 | 1.296 | 0.724 | 0.559 |
| 2-1-0.4* | 0.40 | 3.50 | 1.75 | 0.500 | 480 | 478 | 880 | 1.013 | 0.545 | 0.543 |
| 3-1-0.4* | 0.40 | 3.88 | 1.38 | 0.356 | 700 | 468 | 878 | 1.496 | 0.797 | 0.533 |
| 1-1-0.5* | 0.50 | 4.00 | 2.25 | 0.562 | 640 | 524 | 960 | 1.221 | 0.667 | 0.546 |
| 2-1-0.5 | 0.50 | 3.81 | 1.38 | 0.362 | 600 | 466 | 954 | 1.288 | 0.629 | 0.488 |
| 3-1-0.5* | 0.50 | 3.88 | 1.88 | 0.485 | 660 | 527 | 956 | 1.252 | 0.690 | 0.551 |
| 1-1-0.6* | 0.60 | 3.75 | 2.00 | 0.532 | 480 | 606 | 1036 | 0.792 | 0.463 | 0.585 |
| 2-1-0.6* | 0.60 | 3.56 | 1.56 | 0.438 | 600 | 551 | 1032 | 1.089 | 0.581 | 0.534 |
| 3-1-0.6 | 0.60 | 3.94 | 1.88 | 0.477 | 780 | 523 | 1037 | 1.491 | 0.752 | 0.504 |
| 1-1.4-0.4 | 0.40 | 5.12 | 3.00 | 0.585 | 680 | 1288 | 1635 | 0.528 | 0.416 | 0.788 |
| 2-1.4-0.4 | 0.40 | 5.50 | 3.25 | 0.590 | 880 | 1241 | 1636 | 0.710 | 0.538 | 0.759 |
| 3-1.4-0.4 | 0.40 | 4.75 | 2.50 | 0.526 | 880 | 1122 | 1634 | 0.784 | 0.539 | 0.687 |
| 1-1.4-0.5 | 0.50 | 4.50 | 2.25 | 0.500 | 880 | 1170 | 1811 | 0.752 | 0.486 | 0.646 |
| 2-1.4-0.5* | 0.50 | 4.62 | 2.62 | 0.568 | 840 | 1147 | 1813 | 0.732 | 0.463 | 0.633 |
| 3-1.4-0.5* | 0.50 | 5.38 | 3.75 | 0.698 | 780 | 1256 | 1808 | 0.621 | 0.431 | 0.695 |
| 1-1.4-0.6* | 0.60 | 6.00 | 3.00 | 0.500 | 920 | 1180 | 1966 | 0.780 | 0.468 | 0.600 |
| 2-1.4-0.6 | 0.60 | 5.18 | 2.50 | 0.786 | 940 | 1285 | 1964 | 0.732 | 0.479 | 0.654 |
| 3-1.4-0.6* | 0.60 | 5.75 | 3.00 | 0.522 | 800 | 1209 | 1966 | 0.662 | 0.407 | 0.615 |

*Measured value of c obtained by adding twice the horizontal projection of the bottom crack to cθ (See Reference 12).

$T_{theo}$ - ultimate torque obtained by Lessig's theory, in in-lbs.

B). Comparison and Analysis of Test Results with Theoretical Results

From Table 6, it can be seen that the difference in cross-sectional area of the beams will influence the ultimate load cell readings significantly. The variation of p was expected to be significant in each individual area groupings. It was found that this was not true in the tests.

The crack pattern, according to Mason's report, did not follow the type that Lessig defined. Thus some difficulties were induced in measuring the magnitudes of "c" as used in Lessig's equations. The beams involved in these difficulties are marked by asterisks in Table 6.

Lessig's theory over-estimated the ultimate torsional resistance for both 1x2-inch beams and 1.41x2.83-inch beams in these tests. It is interesting to note that if the reinforcement were increased beyond a certain critical amount, the beams would fail through the crushing of the concrete. The ultimate torsional resistances for this case, calculated by using equation (20), are lower than the torques measured for the 1x2-inch beams as well as the theoretical values for both beam size-groupings. This means that equation (20) is not valid for all cases. Otherwise, it would follow that increasing the amount of reinforcement would correspond to a decreasing torsional resistance of the beam.

The computation of the ultimate torsional resistance using Hsu's theory is presented in Appendix II. The results are tabulated in Table 8. Two figures having $b_{1c}h_{1c}A_{vs}f_{vy}/s$ versus torque were constructed for comparison of the experimental results and the theoretical results of Hsu's theory as well as Lessig's theory, those are Fig. 10 and Fig. 11 for 1x2-inch beams and 1.41x2.83-inch beams respectively. It can be seen from these figures that Hsu's theory results in strength predictions which are considerably lower than those of Lessig's theory and that they are in closer agreement with Mason's experimental results than is Lessig's theory. Taking 1x2-inch beams for example, the average of the ratios of $T_u/T_{actu}$ for Lessig's theory is 1.539 whereas it is 1.087 for Hsu's theory. However, both theories tend to over-estimate the torsional resistance of 1.41x2.83-inch beams as determined experimentally by Mason.

In Hsu's experiment (10), beam series G and series N have the same height-to-width ratio and the same value of "m". However, the slope "K'" for series G is 1.45 and the slope for series N is 1.30 (See Fig. 10-13, Reference 10). This might tend to indicate that the slope for a small beam is smaller. The slope of the curves for both beam size groupings having the same value of p, constructed by Hsu's theory, are essentially identical in this test. But according to the results calcu-

TABLE 8 THE ACTUAL FAILURE TORQUE AND THE ULTIMATE TORQUE CALCULATED BY HSU'S THEORY

| Beam No. | p | $A_{vs}$ sq.in. | s in. | $b_{1c}$ in. | $h_{1c}$ in. | $f'_c$ psi. | $h_{1c}/b_{1c}$ | m | $mf_y/f_{vy}$ | $T_u$ in-lbs | $T_{actu}$ in-lbs | $\frac{T_u}{T_{actu}}$ | $\frac{b_{1c}h_{1c}A_{vs}f_{vy}}{s}$ |
|---|---|---|---|---|---|---|---|---|---|---|---|---|---|
| 1-1-0.4 | 0.4 | 0.004 | 0.3535 | 0.68 | 1.40 | 2895 | 2.059 | 0.319 | 1.202 | 620.0 | 640.0 | 0.969 | 245.6 |
| 2-1-0.4* | 0.4 | 0.004 | 0.3535 | 0.68 | 1.40 | 2820 | 2.059 | 0.319 | 1.202 | 616.6 | 480.0 | 1.285 | 245.6 |
| 3-1-0.4* | 0.4 | 0.004 | 0.3535 | 0.68 | 1.40 | 2790 | 2.059 | 0.319 | 1.202 | 623.3 | 700.0 | 0.890 | 245.6 |
| 1-1-0.5* | 0.5 | 0.004 | 0.2828 | 0.68 | 1.40 | 2805 | 2.059 | 0.255 | 0.962 | 657.6 | 640.0 | 1.028 | 307.0 |
| 2-1-0.5 | 0.5 | 0.004 | 0.2828 | 0.68 | 1.40 | 2715 | 2.059 | 0.255 | 0.962 | 653.5 | 600.0 | 1.089 | 307.0 |
| 3-1-0.5* | 0.5 | 0.004 | 0.2828 | 0.68 | 1.40 | 2745 | 2.059 | 0.255 | 0.962 | 654.9 | 660.0 | 0.992 | 307.0 |
| 1-1-0.6* | 0.6 | 0.004 | 0.2357 | 0.68 | 1.40 | 2865 | 2.059 | 0.212 | 0.801 | 702.1 | 480.0 | 1.463 | 368.4 |
| 2-1-0.6* | 0.6 | 0.004 | 0.2357 | 0.68 | 1.40 | 2810 | 2.059 | 0.212 | 0.801 | 699.6 | 600.0 | 1.166 | 368.4 |
| 3-1-0.6 | 0.6 | 0.004 | 0.2357 | 0.68 | 1.40 | 2875 | 2.059 | 0.212 | 0.801 | 702.5 | 780.0 | 0.900 | 368.4 |
| 1-1.4-0.4 | 0.4 | 0.004 | 0.5793 | 0.93 | 1.69 | 2815 | 1.817 | 0.829 | 1.345 | 1456.0 | 680.0 | 2.145 | 575.2 |
| 2-1.4-0.4 | 0.4 | 0.004 | 0.5793 | 0.93 | 1.69 | 2845 | 1.817 | 0.829 | 1.345 | 1462.2 | 880.0 | 1.661 | 575.2 |
| 3-1.4-0.4 | 0.4 | 0.004 | 0.5793 | 0.93 | 1.69 | 2785 | 1.817 | 0.829 | 1.345 | 1455.8 | 880.0 | 1.654 | 575.2 |
| 1-1.4-0.5 | 0.5 | 0.004 | 0.4634 | 0.93 | 1.69 | 2825 | 1.817 | 0.663 | 1.076 | 1546.3 | 880.0 | 1.757 | 718.9 |
| 2-1.4-0.5* | 0.5 | 0.004 | 0.4634 | 0.93 | 1.69 | 2860 | 1.817 | 0.663 | 1.076 | 1550.0 | 840.0 | 1.845 | 718.9 |
| 3-1.4-0.5* | 0.5 | 0.004 | 0.4634 | 0.93 | 1.69 | 2755 | 1.817 | 0.663 | 1.076 | 1538.8 | 780.0 | 1.973 | 718.9 |
| 1-1.4-0.6* | 0.6 | 0.004 | 0.3862 | 0.93 | 1.69 | 2795 | 1.817 | 0.553 | 0.897 | 1629.3 | 920.0 | 1.771 | 862.7 |
| 2-1.4-0.6 | 0.6 | 0.004 | 0.3862 | 0.93 | 1.69 | 2760 | 1.817 | 0.553 | 0.897 | 1625.5 | 940.0 | 1.729 | 862.7 |
| 3-1.4-0.6* | 0.6 | 0.004 | 0.3862 | 0.93 | 1.69 | 2800 | 1.817 | 0.553 | 0.897 | 1629.9 | 800.0 | 2.037 | 862.7 |

* See Reference 12.

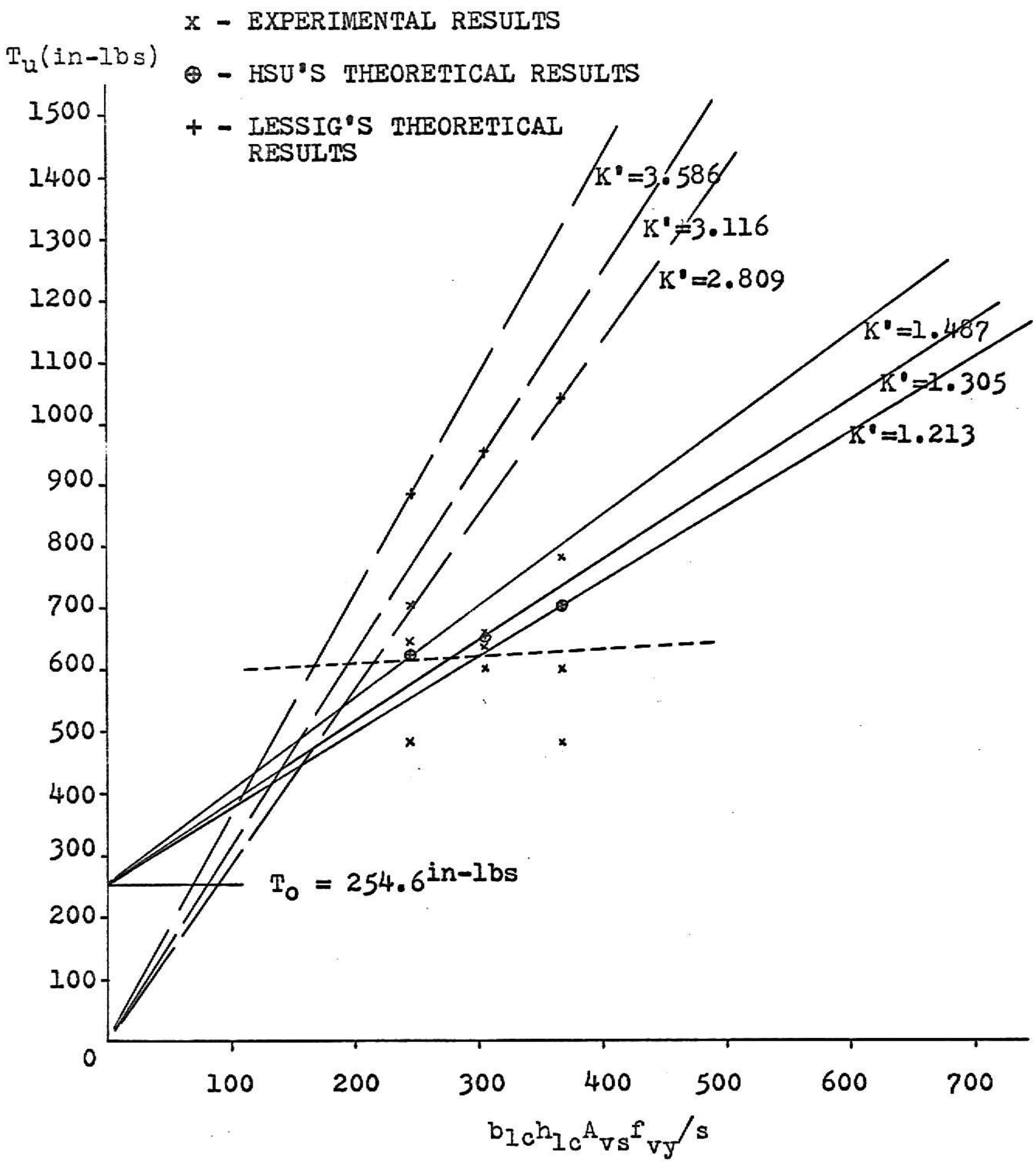


FIG. 10 - COMPARISON OF EXPERIMENTAL RESULTS WITH THEORETICAL RESULTS FOR 1x2-in. BEAMS

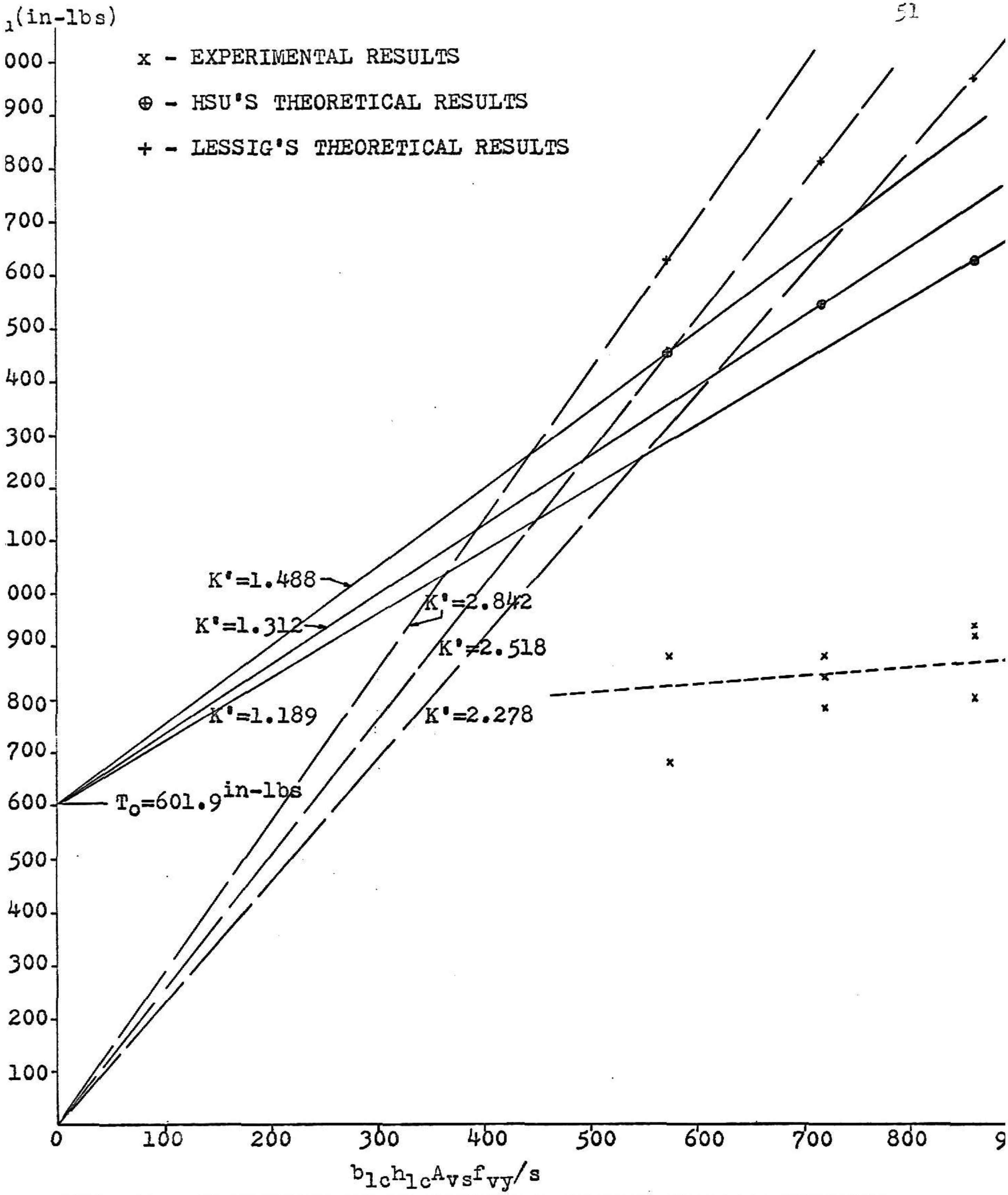


FIG. 11 - COMPARISON OF EXPERIMENTAL RESULTS WITH THEORERICAL RESULTS FOR 1.41x2.83-in. BEAMS

lated by Lessig's theory, the curves for the larger beams in this test had a smaller slope. It is suggested that some investigations of the effect of the beam size on the slopes of the design curves should be undertaken. The effect of beam size on the value of K' may not be significant for prototype tests due to the small variations in the beam sizes. Nevertheless, it could be important in model tests since the sizes of models are much smaller than their prototypes. In other words, the slopes of the curves may differ considerably between the models and their prototypes. If this is true, the design equation for prototypes will not be valid for models unless some modifications are made to take into account the size effect. Comparing the design equations of the two theories, the slope of the curves constructed using equation (15) are affected by the beam size, whereas equation (55) will yield the same slope as long as the ratios $m \cdot f_y/f_{vy}$ and $h_{1c}/b_{1c}$ are identical.

The curves plotted by Lessig's theory in Fig. 10 and Fig. 11 are considerably steeper than that of Hsu's theory. While Hsu's curves seem to fit the data points in Fig. 10 a little better than Lessig's, it is difficult to tell as to which one is more reasonable because only one point was obtained for each curve.

The dotted lines in Fig. 10 and Fig. 11 are the best fit for the measured torques. The fact that these lines are almost horizontal indicates that the variation of p had little effect on the ultimate torque for beams of the same size groupings. This phenomena was not expected since these beams were reinforced purposely to obtain a variation in the ultimate torque. It is assumed that there were some mistakes involved in the fabrication or testing of the beams since the test results differed considerably within batches. This assumption may also be indicated by the fact that the 1.41 x 2.83-inch beams had about twice the cross-sectional area and reinforcement of the 1x2-inch beams but the torsional capacities of the two size groupings were not much different.

It was expected in both theories that the beam would continue to take load after the initial tension cracks started. Furthermore, Hsu stated that the behavior after initial cracking should be much different from the behavior before initial cracking. In Mason's tests (12), the load dropped off immediately after the initial cracks occured and continue to drop until the beam failed. The reason for this phenomena is unclear. Over-reinforcement of the beams is suggested by the fact that the failure torques measured in the tests were almost constant within the same area grouping and, according to Lessig's theory, the torsional capacities of the 1x2-inch beams calculated by equation (20) are smaller than the results of equation (15). However, this is not the case since the total volume percentage of reinforcement is smaller than the balanced percentage defined in both theories.

Inability to simulate the properties of the actual materials by the model materials could also have influenced the test results. Mason pointed out that the two types of smooth wire used as transverse reinforcement in this test had many undesirable properties(12). The black annealed wire used in the smaller torsion specimens was extremely soft and exhibited a low yield point. Lack of bond by using smooth wire as reinforcement should also be considered. Poor bond stress could prevent the reinforcement from reaching it's yield stress at failure. This might also explain the fact that the beams under testing failed to behave as described in either Lessig's theory and Hsu's theory. Since no tests were devoted to the determination of the bond stresses for these wires, an analysis of this variable was not possible.

The 1x2-inch beams had a closer agreement between the theoretical results and the experimental results, especially for Hsu's theory. This does not necessarily indicate that Hsu's theory is applicable to these beams, since these beams were reinforced with only two longitudinal bars, rather than four, which was the case considered by Hsu.

## GENERAL CONCLUSIONS

Extensive research and experiments on the behavior of reinforced concrete beams subjected to torque have been undertaken. The Andersen-Cowan theory, the most widely accepted theory in the past, was based on Saint-Venant's theory and treated the reinforced concrete as an isotropic material. More compatible theories based on ultimate torsional strength of the reinforced concrete rectangular beams have been developed. These theories can exhibit the real load-bearing capacities of the beams.

Two theories dealing with the ultimate torsional strengths of beams were reviewed, Lessig's theory and Hsu's theory. The derived design equations for both theories had essentially the same form as those of the German and Australian codes.

Lessig's theory considers the combined effects of torsion, flexure moment and transverse forces. Two modes of failure were proposed and the surfaces of failure for both modes were assumed to be spiral shaped. For pure torsion, the neutral axis passes through both horizontal sides of the beam. The dowel forces are not considered.

Hsu's theory proposes a failure plane perpendicular to both vertical sides of the beam and inclined $45^\circ$ to the beam axis. Thus, the horizontal stirrups are not assumed to contribute to the torsional resistance of the beam. The dowel forces are considered in his theory. The final design equations were derived from empirical data since some of the coefficients could not be obtained by theoretical investigations because of insufficient information.

The results from Mason's small scale model test were used to compare with these two theories. In Mason's experiments, two sizes of model beams were tested. The material adopted as a substitution for concrete, longitudinal reinforcement and transverse reinforcement were Ultracal-30 mix, #6-32 threaded rod and smooth wire respectively. The properties of these substituting materials simulated their prototypes satisfactorily. However, the experimental results were considerably lower than those predicted by Lessig's theory or by Hsu's theory. Hsu's theory had a better agreement with the test results but the comparison is still unfavorable. It is believed that there were probably some mistakes induced in the fabrication or testing of the beams. If not, either a modification of the theories is necessary or the simulation of a model and its prototype can not be considered as linear for reinforced concrete beam models loaded in torsion.

# RECOMMENDATIONS FOR FURTHER RESEARCH

To the best of our knowledge in the field of the concrete strength theory, the torsional capacity of a reinforced concrete beam which fails through the failure of the concrete is still mainly obtained through the use of empirical equations. In Hsu's theory, a maximum limitation was given to the total steel-concrete volume percentage to assure that the beam would not fail through the crushing of the concrete. For beams having larger percentages of reinforcement than the limiting value, the excessive reinforcement is simply ignored. In Lessig's theory, an empirical equation was given for this case. More extensive theoretical and experimental investigations on the behavior of this type of failure should be undertaken.

Equation (54), which is an extension of equation (53), covers beams reinforced with different grades of longitudinal and transverse steel. This equation is not yet affirmed by substantially experimental data (11). Thus, equation (55) should be justified by more tests for cases where $m \neq 1$.

The dowel-force actions for both longitudinal steel and stirrups are not clear. Tests revealed that they are affected by the cross-sectional area and the distortion of the reinforcing bars. They are also affected by the spacing of the stirrups. The quantities of these forces can not be accurately evaluated at present. More information is needed.

A square section is usually considered as a special case of rectangular sections. However, it was found that a square beam subjected to torsion would form a different type of crack pattern than a rectangular section would have (11). A study to determine the relationship between the square section and the rectangular section should be undertaken.

In the small scale model tests discussed, more accurate results could have obtained if a more sensitive load cell had been used. Furthermore, more detailed and more successful analyses in the model tests could have been achieved if the models had been instrumented for measurement of the plaster and reinforcement strains. Further model tests should be able to resolve the questions relating to size effects on Hsu's theory.

## LIST OF SYMBOLS

$M$ - flexure moment applied to a beam, in-lbs.

$M_o$ - moment about the neutral axis, in-lbs.

$T$ - twisting moment applied to a beam, in-lbs.

$Q$ - shear force applied to a beam, in-lbs.

$l$ - length of the neutral axis at the surface of failure, in.

$l'$ - projection of $l$ on the vertical face of the beam, in.

$c$ - length of the horizontal projection of $l$ in a direction along the beam axis, in.

$x$ - horizontal measurement of the concrete compression zone at the surface of failure, in.

$x_1$ - see Fig. 3b.

$x_2$ - see Fig. 3b.

$\xi$ - a variable introduced for integration.

$h$ - over-all dimension of the beam height, in.

$h'$ - see page 10.

$b$ - over-all dimension of the beam width, in.

$b_1$ - distance from the center of the vertical stirrups to the nearer vertical face of the beam, in.

$b_o$ - distance from the center of the vertical stirrups to the farther vertical face of the beam, in.

$b_2$ - distance from the center of the longitudinal steel to the nearer vertical face of the beam, in.

$h_1$ - distance from the center of the horizontal stirrups to the nearer horizontal face of the beam, in.

$h2$ - distance from the center of the longitudinal steel to the nearer horizontal face of the beam, in.

$\theta$ - a non-dimensional coefficient, see Fig. 3a.

$\alpha$ - angle between the cracks on horizontal faces of the beam and the beam axis, radians.*

$s$ - center-to-center spacing of the stirrups, in.

$S_b$ - statical moment of the compression area about the neutral axis.

$f_c$ - ultimate strength of concrete, psi. See page 7.

$f'_c$ - cylinder compressive strength of concrete, psi.

$f_t$ - tensile strength of concrete, psi.

$f_y$ - tensile yielding strength of the longitudinal steel, psi.

$f_{vy}$ - tensile yielding strength of the stirrup steel, psi.

$A_s$ - area of the longitudinal steel on one side of the beam, $in^2$.

$A'_s$ - cross-sectional area of the longitudinal bars within the shear-compression zone, $in^2$.

$A_{vs}$ - cross-sectional area of one stirrup, $in^2$.

$p$ - a coefficient, see page 12.

$z$ - distance from the center of the longitudinal bars in the tension area to the center of the concrete compression zone.*

$y$ - a coefficient, see page 13.

$k$ - a coefficient obtained from experimental data, see page 15.

$T_{up}$ - ultimate torque applied to the plain concrete rectangular beam, in-lbs.

* Lessig's theory.

$T_{cr}$ - the torque when beam cracking was first seen on the concrete surface, in-lbs.

$T_u$ - ultimate torque of reinforced concrete members, in-lbs.

$T'$ - resisting torque provided by the shear strength of the concrete in the shear-compression zone, in-lbs.

$T_o$ - value of $T_u$ where a $T_u$ versus $b_{1c}h_{1c}A_{vs}f_{vy}/s$ curve intercepts the vertical coordinate, in-lbs.

$\phi$ - angle between the assumed failure surface and the beam axis, radians.**

$f_r$ - modulus of rupture of concrete, psi.

K - ratio between the modulus of rupture and the tensile strength.

$p_{tb}$ - balanced total volume percentage of reinforcement, in percentage.

$p_t$ - the percentage of total steel by volume in the concrete beam, in percentage.

$h_{1c}$ - larger center-to-center dimension of a closed rectangular stirrup, in.

$h_{2c}$ - vertical center-to-center distance between the longitudinal corner bars, in.

$b_{12}$ - distance from the center of a stirrup to the nearest center of longitudinal corner bars, in.

$b_{1c}$ - distance from the center of the longer leg of stirrups outside the shear-compression zone to the center of shear-compression zone, in.**

** Hsu's theory.

$d_{1t}$ - distance between the center of the vertical stirrups in the tensile zone and the axis of twist, in.

$d_{2t}$ - horizontal distance between the center of the longitudinal bars in the tensile zone and the axis of twist, in.

$d_{ct}$ - distance from the center of the shear-compression zone to the axis of twist, in.

$F_h$ - horizontal dowel force of one longitudinal corner bar in the tension zone, lbs.

$F_v$ - vertical dowel force of one longitudinal corner bar in the tension zone, lbs.

$P$ - vertical force-component on the shear-compression zone, lbs.

$P_s$ - shear force of the concrete on the shear-compression zone, lbs.

$P_l$ - tensile force of the longitudinal bars in the shear-compression zone, lbs.

$P_c$ - concrete compressive force perpendicular to the shear-compression zone, lbs.

$\lambda$ - an efficiency coefficient, see page 27.

m - ratio of volume of longitudinal bars to volume of stirrups.

q - dowel stresses per unit displacement, in in-lb per cu.in., a constant.

$\bar{\theta}$ - relative angle of twist of the two surfaces of the failure crack, in radians, roughly a constant.

$v_{av}$ - average shear stress in the shear-compression zone, psi.

$v_c'$ - pure shear strength of concrete, psi.

$k_1$ - ratio between $v_{av}$ and $v_c'$.

$k_2$ - ratio between x and b.

K' - slope of a $T_u$ versus $b_{1c}h_{1c}A_{vs}f_{vy}/s$ curve.

E - modulus of elasticity, psi.

$T_{actu}$ - actual failure torque determined from load cell readings, in-lbs or ft-lbs.

$T_{calc}$ - ultimate torque calculated by Lessig's theory using the measured parameters.

$T_{theo}$ - ultimate torque obtained by Lessig's theory.

$T_e$ - permissible torque calculated by elastic theory.

## ACKNOWLEDGEMENTS

The author wishes to express his most sincere gratitude to Dr. Robert R. Snell, his faculty advisor, for offering valuable advice, constant encouragement and for reviewing the preliminary manuscript.

Acknowlegements are also given to Mr. Jerry Liu and Mr. John Yen for the kind assistance they rendered to the author.

# BIBLIOGRAPHY

1. Andersen, P., "Experiments with Concrete in Torsion," Transactions, ASCE, Vol. 100, Paper No. 1912, 1935. pp. 949-983.
2. Cowan, H. J., "Elastic Theory for Torsional Strength of Rectangular Reinforced Concrete Beams," Magazine of Concrete Research, Vol. 2, No. 4, London, England, July 1950. pp.3-8.
3. Cowan, H. J., "Design of Beams Subjected to Torsion Related to the New Australian Code," Journal of the American Concrete Institute, Vol. 31, No. 7, January 1960. pp. 591-618.
4. Lessig, N. N., "Determination of the Load-Carrying Capacity of Reinforced Concrete Elements with Rectangular Cross-Section under Simultaneous Action of Flexure with Torsion," Benton i Zhelezobeton, No. 3, 1959, pp. 109-113. (Foreign Literature Study No. 348.)*
5. Lessig, N. N., "Determination of the Load-Carrying Capacity of Reinforced Concrete Elements with Rectangular Cross-Section Subjected to Flexure with Torsion," No. 5, 1959, pp. 5-28. (Foreign Literature Study No. 371.)*
6. Lessig, N. N., "Study of Cases of Failure of Concrete in Reinforced Concrete Elements with Rectangular Cross-Section Subjected to Combined Flexure and Torsion," Design of Concrete Structures, State Publishing Office of Literature on Structural Engineering, Architecture, and Structural Materials, Moscow. (Foreign Literature Study No. 398.)*

* Portland Cement Association, Research & Development Library, SKOKIE, ILL.

7. Yu. V. Chinenkov, "Study of the Behavior of Reinforced Concrete Elements in Combined Flexure and Torsion," Trudy, No. 5, 1959, pp.29-53. (Foreign Literature Study No. 370.)*

8. Hsu, T. T. C., "Torsion of Structural Concrete - A Summary on Pure Torsion," Symposium on Torsion, SP No. 18, American Concrete Institute, Detroit, 1968. pp.165-178.

9. Hsu, T. T. C., "Torsion of Structural Concrete - Plain Concrete Rectangular Sections," Symposium on Torsion, SP No. 18, American Concrete Institute, Detroit, 1968. pp.203-238.

10. Hsu, T. T. C., "Torsion of Structural Concrete - Behavior of Reinforced Concrete Rectangular Members," Symposium on Torsion, SP No. 18, American Concrete Institute, Detroit, 1968. pp.261-306.

11. Hsu, T. T. C., "Ultimate Torque of Reinforced Rectangular Beams," Proceedings, ASCE, Vol. 94, No. ST3, February 1968.

12. Gary E. Mason, "Small Scale Model Analysis of Reinforced Concrete Beams in Flexure and in Torsion," Master's Thesis, Department of Civil Engineering, Kansas State University, 1967.

13. Timoshenko, S., Strength of Materials, 3rd Edition, Part II, D. Van Nostrand Co., Inc., Princeton, N. J., 1956. p.459.

* Portland Cement Association, Research & Development Library, SKOKIE, ILL.

# APPENDIX I

TABLE I-1 COMPARISON OF ELASTIC THEORY AND THE HSU'S THEORY FOR ULTIMATE TORQUE

| Beam | Experimental Ultimate Torque, $T_{actu}$"k | Elastic Theory | | Hsu's Theory | | $\frac{b^2h}{3}0.85f_t$ | $\frac{f_r}{f_t}$ | |
|---|---|---|---|---|---|---|---|---|
| | | $T_e$"k | $\frac{T_{actu}}{T_e}$ | $T_u$"k | $\frac{T_{actu}}{T_u}$ | | | |
| A1 | 162 | 122 | 1.33 | 166 | 0.98 | 151 | 1.07 | |
| A2 | 169 | 122 | 1.39 | 166 | 1.02 | 151 | 1.12 | |
| A3 | 102 | 76.3 | 1.34 | 101 | 1.01 | 92 | 1.11 | |
| A4 | 100 | 76.3 | 1.31 | 101 | 0.99 | 92 | 1.08 | Average 1.10 |
| A5 | 216 | 169 | 1.28 | 214 | 1.01 | 195 | 1.11 | |
| A6 | 216 | 170 | 1.27 | 217 | 0.99 | 196 | 1.10 | |
| A7 | 54 | 33.6 | 1.61 | 53.2 | 1.02 | 39.8 | 1.36 | |
| A8 | 56.5 | 33.6 | 1.68 | 53.2 | 1.06 | 39.8 | 1.42 | Average 1.34 |
| A9 | 101 | 68.5 | 1.48 | 96.5 | 1.05 | 71.7 | 1.41 | |
| A10 | 85 | 64.1 | 1.33 | 90.2 | 0.94 | 67.1 | 1.27 | |
| Average | | | 1.40 | | 1.01 | | | |

Details are reported in Reference 9.

TABLE I-2

COMPARISON OF CALCULATED VALUE OF $T_o$ AND $\lambda$ WITH TEST RESULTS

| Beam Series Designation | Test Results | | Equation 50 | Equation 53 |
|---|---|---|---|---|
| | $T_o$, "k | K' | $T_o$, "k | K' |
| B | 75 | 1.20 | 74 | 1.20 |
| D | 75 | 1.20 | 74 | 1.20 |
| M | 75 | 1.70 | 74 | 1.56 |
| I | 95 | 1.37 | 92 | 1.20 |
| J | 60 | 1.20 | 54 | 1.20 |
| G | 95 | 1.45 | 98 | 1.38 |
| N | 30 | 1.30 | 28 | 1.38 |
| K | 45 | 1.50 | 45 | 1.52 |
| C | 50 | 0.95 | 49 | 0.99 |

Details are reported in Reference 10.

# APPENDIX II

```
C   C  ULTIMATE TORQUE CALCULATED BY THE THEORY OF LESSIG
       DO 100 I=1,2
       READ 1, B,H,B1,H1,BO
       READ 1,FVY,AVS,FY,AS
       DO 100 M=1,9
       READ 1, P,FC1
     1 FORMAT(5F15.6)
       CA=H/(2.0*B+H)
       C=(B*H/(P*CA))**0.5
       S=(FVY*AVS*B)/(FY*AS*P)
       CMAX=2.0*B+H
       PUNCH 1, CA,C,S
       DO 20 N=1,3
       IF (C-CMAX)11,11,10
    10 C=CMAX
    11 X1=(AS*FY*H+AVS*FVY*(C**2.0)*CA/S)
       X=X1/(0.85*FC1*(C**2.0+H**2.0))
       Z=BO-0.5*X
       Y=CA*(B-B1-0.5*X)+(1.0-CA)*(0.25*H*(1.0-CA)-H1)
       PUNCH 1, X,Z,Y
       C=(Z*B*H/(P*Y))**0.5
       PUNCH 1,C
    20 CONTINUE
       T=AS*FY*H*(Z+P*(C**2.0)*Y/(B*H))/C
       PUNCH 1, T
   100 CONTINUE
       STOP
       END
```

```
C   C  THE ULTIMATE TORQUE CALCULATED BY USING THE THEORY OF HSU
       DO 100 I=1,18
       READ 1,AVS,AS,FVY,FY,B,P
     1 FORMAT (6F10.4)
       S=(AVS*FVY*B)/(P*AS*FY)
       PUNCH 2,S
     2 FORMAT (F10.6)
       READ 1,H,FC,H1C,B1C
       HBR=H1C/B1C
       PUNCH 2,HBR
       IF(HBR-2.6)11,13,10
    10 HBR=2.6
       GO TO 13
    11 IF(HBR-1.5)12,13,13
    12 PUNCH 3
     3 FORMAT(16HUNPROPER SECTION)
    13 T1=2.4*(B**1.5)*H*(FC**0.5)
       RM=AS*S/(AVS*(B1C+H1C))
       PUNCH 2,RM
       F=RM*FY/FVY
       IF(F-1.5)22,31,21
    21 F=1.5
       GO TO 31
    22 IF(F-0.7)23,31,31
    23 RM=0.7*FVY/FY
       AVS=AS*S/(RM*(B1C+H1C))
       F=0.7
    31 PUNCH 2,F
       PTB=2400.0*(FC**0.5)/FVY
       PS=2.0*(AS+(AVS*(H1C+B1C)/S))/(B*H)
       IF(PS-PTB)41,41,40
    40 AS=AS*PTB/PS
       AVS=AVS*PTB/PS
    41 C1=0.66*F+0.33*HBR
       C2=B1C*H1C*AVS*FVY/S
       PUNCH 2,C2
       T2=C1*C2
       TU=T1+T2
       PUNCH 1,TU
       READ 2,TA
       RT=TU/TA
       PUNCH 2,RT
   100 CONTINUE
       STOP
       END
```

# A STUDY OF THE TORSIONAL CAPACITY OF REINFORCED CONCRETE RECTANGULAR BEAMS

by

JOSEPH CHIA-HUA CHU

B.S. in C.E., Taiwan Provincial Taipei Institute of Technology
1965

---

AN ABSTRACT OF A MASTER'S REPORT

submitted in partial fulfillment of the

requirements for the degree

MASTER OF SCIENCE

Department of Civil Engineering

KANSAS STATE UNIVERSITY
Manhattan, Kansas

1970

# ABSTRACT

The purpose of this report was to study two theories concerning the ultimate torsional resistance of reinforced concrete rectangular beams and to compare these theories with the results of some small scale model tests in an attempt to determine whether the plaster model tests could verify the results predicted by either theory. The theories reviewed were Lessig's theory and Hsu's theory. Both theories have the governing equations derived on the basis of assuming a failure surface from experimental observations.

The experiments carried out by Mason were designed for a range of cross-section-p combinations. The materials used in these tests simulated the properties of their prototypes satisfactorily. By comparison of the test results with the theoretical results of the two theories studied, it was found that the experimental values did not agree well with either of the theories. The reasons for this result are unclear. Further research is needed to examine whether plaster model tests are applicable to the investigation of the torsional behavior of reinforced concrete beams.